In the reply, the referee's comments are in *italics*, our response is in normal text, quotes and modifications from the manuscript are in blue.

Anonymous Referee #1

This paper presents a modelling study of Jakobshavn Isbrae using the ice flow model BISICLES. The model is initialised and calibrated to fit the observed front retreat and annual velocities between 2004 and 2013. Three parametrisations are used to control the position of the front:

• basal melting (Eq. 11),

• calving based on a crevasse depth criteria (Eq. 10),

• and a parametrisation meant to represent the buttressing of the ice melange in the front and that affect the driving stress (Eqs. 8-9) near the front.

Because it is a target for the calibration, the total observed front retreat is well reproduced by the model. The timing of the front variations with winter advance and summer retreat is captured by the model, however the seasonal variability is overestimated at the end of the period because the model does not reproduce the winter calving. Finally, the model is used to estimate the evolution during the 21st century. The results during the calibration are convincing and well discussed. However, I found that few points are missing for the description of the model and set-up, the initialization and calibration is relatively hard to follow as it involves many steps that have been implemented manually and the discussion mainly concentrates on what the model has and forget to include what is missing. I give more details below.

My main remark concerns the parametrisation of the buttressing by the ice melange. The boundary condition for the front is not mentioned in the model description but should be the difference between the force exerted by the ice and the back stress from the sea water.

Reply: Yes you are right. We added boundary conditions into text:

Reflection boundary conditions were applied at the edge of each domain:

$$\boldsymbol{u}\cdot\boldsymbol{n}=0, \qquad \boldsymbol{t}\cdot\nabla\boldsymbol{u}\cdot\boldsymbol{n}=0, \qquad \nabla h\cdot\boldsymbol{n}=0, \quad (8)$$

where $\boldsymbol{n}$ is normal to a boundary and $\boldsymbol{t}$ is parallel to it. Normal stress across the calving front is equal to the hydrostatic water pressure there:

$$\boldsymbol{n}\cdot[\phi h\bar{\mu}(2\dot{\boldsymbol{\epsilon}}+2\mathrm{tr}(\dot{\boldsymbol{\epsilon}})\mathbf{I})]-\boldsymbol{\tau}^b=\frac{1}{2}\rho_i g\left(1-\frac{\rho_i}{\rho_w}\right)h^2\boldsymbol{n}. \quad (9)$$

It would seem natural to implement the effect of the ice melange as an additional back stress. The parametrisation implemented here modifies the driving stress near the front. More justification for this implementation is really required.

Reply: Yes that's one way, but our parameterization of ice mélange buttressing is similar to Nick et al., (2013, Eq. S5) which also alters the stress balance at calving front. So our method is established in the literature. We cite Nick in this part.

Is this process really needed to reproduce the front variations? What appends if there is only the calving parametrisation?

Reply: Mélange buttressing effects plays a decisive role in the recent retreating and evolving of Jakobshavn (Joughin et al., 2004; Joughin et al., 2008; Vieli et al., 2011). Ice mélange buttressing does affect calving by altering the stress field that contributes to crevasse penetration depth (Eq. 12). Our buttressing parameterization gives a longitudinal resistance that is 18% of the driving force at the calving front (Eq. 10), for the instance of 2004.

Moreover, the effect is proportional to the fjord temperature and is thus continuously increasing in the future simulations. However, as the temperature increases, we may expect some kind of threshold where the ice melange disappears and its effects become negligible?
Reply: The presence of mélange may scale with temperature to some extent, but it is unlikely to exhibit threshold behavior, because ocean water cannot instantaneously melt ice. Also, increased calving fluxes will oppose ocean warming. These processes are not yet well enough understood for their impact on mélange buttressing to be quantified.

Few important informations are missing for the model description: What is the temperature field for the initialisation? Is the model thermo-mechanically coupled? What is the mesh resolution?
Reply: Our model is not thermo-mechanically coupled with a fixed temperature field -10 °C. Our finest resolution is 500 m which cover the whole fast-flow-area, and we show an example in the new Fig. 1C.

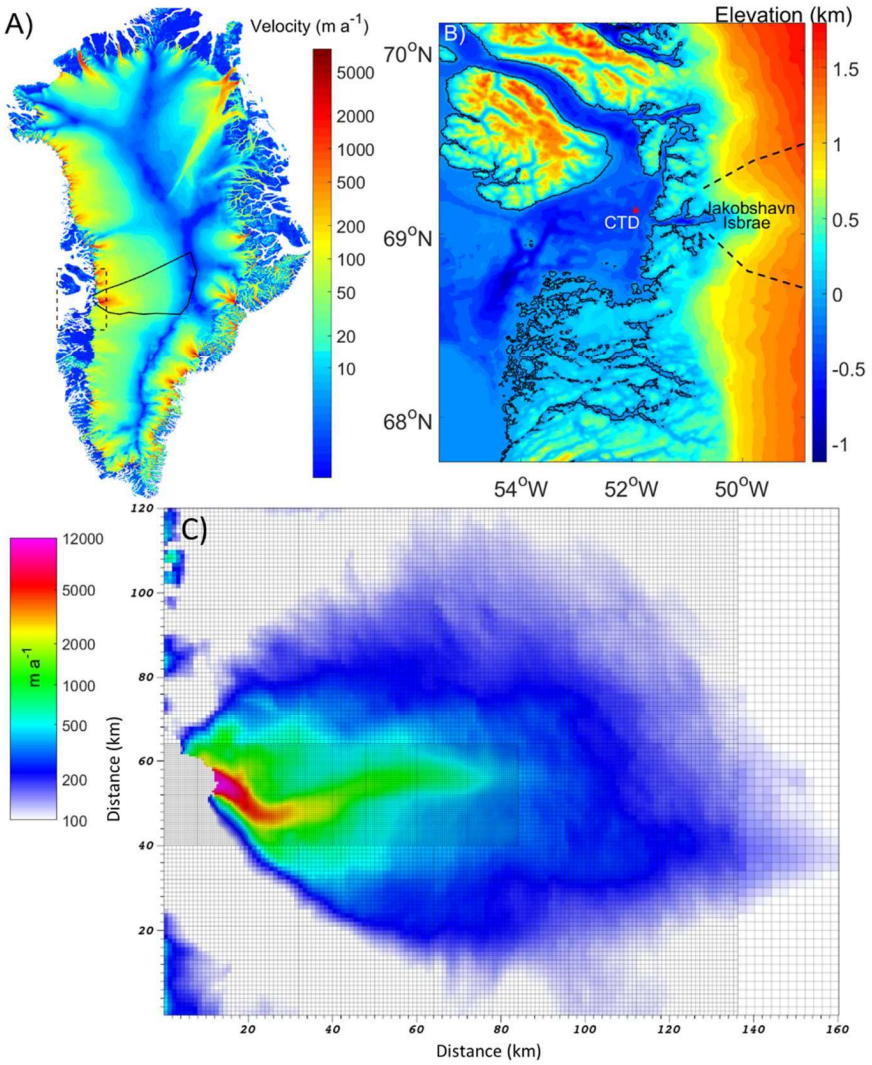

Figure 1. A) Greenland ice sheet flow speeds from Joughin et al. (2018), with the Jakobshavn drainage basin outlined by the solid black line and the area shown in panel B by the dashed box. B) Ilulissat Fjord and Disko Bay bathymetry from Jakobsson et al. (2012), with the CTD (Conductivity Temperature Depth) site used for ocean temperature here marked by the red star. C) Example of the mesh used with finest resolution of 500 m with modeled velocities at the beginning of 2004.

The description of the initialisation is very hard to follow. For example for the step 2, we don't know what is the target to adjust β. In step 3, it is said that β from step 2 is used but that there is no calving, however β controls the calving criteria.

Reply: Agreed, the statement was imprecise. The section 2.3 has been rewritten:

1) We solved the inverse problem for basal conditions (Eq. 7) and stiffening factor using 2010 velocities (Joughin et al., 2010) and 2009 geometry (Gogineni et al., 2012), following Cornford et al. (2015). Our friction coefficient and stiffening factor fields are shown in Fig. 3. Fig. S1 shows the discrepancy between observed velocity field (Joughin et al., 2010) and the velocity derived from the inversion.
2) Starting from the inversion of step 1, we let the model glacier evolve freely without calving and with zero SMB and with sub-shelf melting (γ=0.0238) forced by

repeating the observed 2004 ocean temperature for 11 years until its surface elevation profile reached a state shown in Fig. S2.

3) We carried out several 10-year simulations each with different β values estimated. These simulations were forced by repeatedly applying the 2004 seasonal climate forcing so that the glacier approaches a steady state. From these, we selected the β that provided a calving front position closest to that observed in 2004. The best β here is 0.034. This is our best guess for the 2004 state. The annual minimum extent of Jakobshavn retreats ~ 2 km from 2004 to 2005 following the loss of melange butressing, but then stabilizes until 2007 (Joughin et al. 2010). Annual maximum extents are stable over the 2004-2007 period. Front velocities increase slowly from 2004-2007 (~5.9% a^{-1} Joughin et al. 2010), and the model simulated velocities increase by about 3% a^{-1}. This period of relative stability also makes 2004 a good time from which to start transient simulations.

Basal friction coefficient values downstream of the 2010 grounding line were set equal to that in the nearest 2010 grounded location. This was necessary because steps 2 and 3 involved grounding line advance beyond the region for which basal friction coefficients had been inferred. The geometry after this spin up procedure, and the friction coefficient and stiffening factor distribution from the inversion in step 1 were used as the initial condition for model calibration.

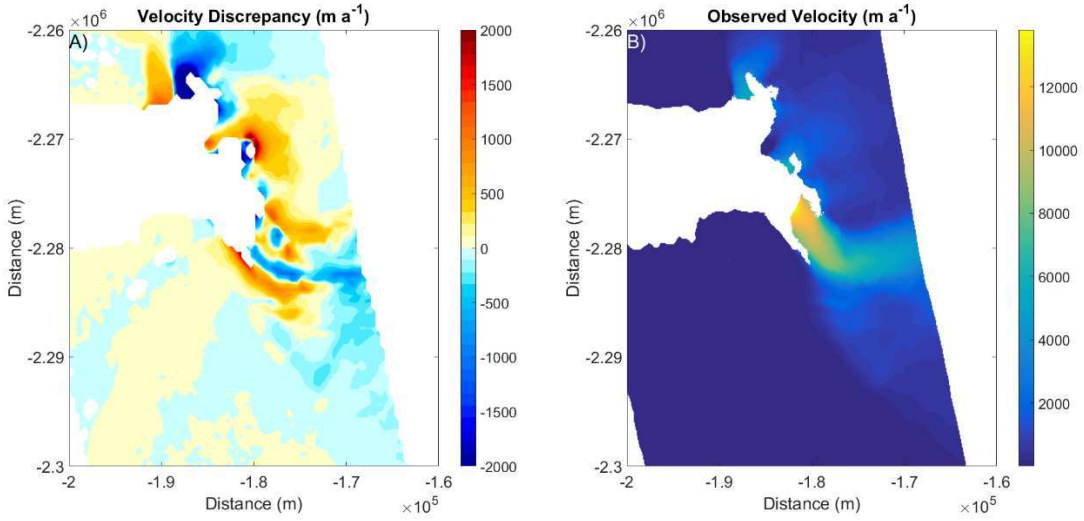

Figure S1. A) Velocity discrepancy (velocity from inversion - observed) and B) the observed velocity field (Joughin et al., 2010).

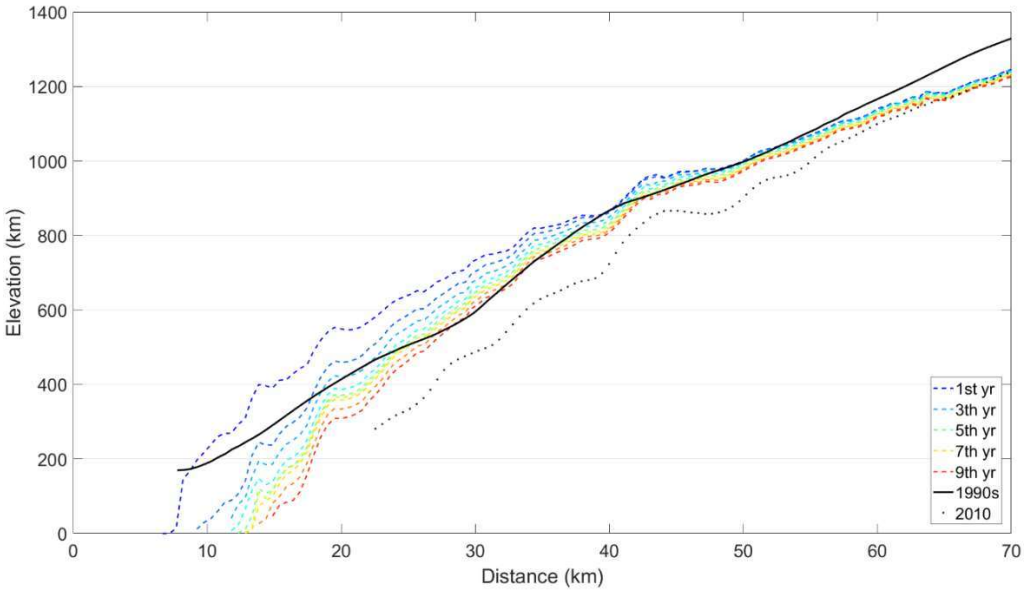

Figure S2. Profiles of surface elevation during the initialization procedure (section 2.3) step 3. Black solid line and black dashed line show the known profiles taken in the 1990s (Bamber et al., 2001) and 2010 (Gogineni et al., 2012) respectively. The profile with legend '1st yr' is the final state of section 2.3 step 2. The profile '7th yr' is the geometry rebuilt for 2004's Jakobshavn, which is the initial state for later simulations.

It is said that γ = 1, however in page 9, Eq. 11, it is said that γ was derived from the 1985 observed submarine melt rate.

Reply: We were unclear and so rewrote this paragraph:

The parameters in the model, α, β and γ representing mélange buttressing, crevasse depth sensitivity to surface runoff, and shelf melt sensitivity to ocean temperatures need to be estimated. The measured relationship between ocean temperatures and sub-shelf melt rate (Motyka et al., 2011) gives the value of γ to be 0.238. We tune parameters α and β manually to best reproduce Jakobshavn Isbræ's calving front position and surface velocity evolution for the 10 year period 2004-2013. Reproducing the total retreat distance and the temporary stable state after 2012 were secondary desirable features to match. The best set of parameters are α_1=0.82, α_2=0.111, β=0.0638. Since these values come from a manual search we do not claim them to be the best in all parameter space. We assess model sensitivity to the parameter values next.

The discussion mainly focuses on the effect of the shear margins and the fact that due to the non linearity in the ice flow law the effective viscosity decreases as the strain-rates increase. This mechanism is described as a positive feedback, however I'm not sure that this is the right term, as both the velocities and the strain-rates are the results of the force balance equation, so that the velocities and the effective viscosity depends on the model parameters and boundary conditions. But is it difficult to describe this as a feedback as they both are solution of the same equation.

Reply: OK, the mechanism is due to the non-linear rheology of the ice, so we change

the text to "This mechanism is due to the non-linear rheology of the ice in the fast flow region".

However, the results are certainly dependent of the ice flow law and the value of the stress exponent, and we certainly may expect that the results would be different with a linear flow relation, or, as discussed, a flow band model that would parametrised the lateral drag.
Reply: Agreed and addressed by the change above.

The mesh resolution might also influence the results as the resolution should be sufficient to properly capture the steep velocity gradients to represent this effect.
Reply: Yes, our finest resolution is 500 m and covers the main trunk and shear margins (Fig. 1C).

In addition, the comparison with Bondzio et al. (2017) might be a bit confusing as Bondzio et al. include the thermo-mechanical coupling (which is absent here?), and they report that the warming from shear heating accounts for 20 to 30% of the decrease in effective viscosity. There is also several mechanisms that could affect the viscosity of the shear margins with potential feedbacks, this includes damage, cryo-hydrologic warming, anisotropy etc... This could be discussed also.
Reply: Agreed. Our model is not thermo-mechanical coupled. The periods used by Bondzio are not are not quite the same as ours. Here we only attempt to roughly verify our results by cross model comparison. We add more discussion in section 4:
Several absent processes in our model could affect ice viscosity. Crevasses saturated by surface melt water within the shear margins of Jakobshavn are visible on satellite images (Lampkin et al., 2013). This melt water can transfer heat throughout the ice column through discharge within crevasses and moulins thus soften the ice (Phillips et al., 2010). Incorporating a continuum damage model in BISICLES would further exaggerate the shear margin weakening as it raises the non-linear dependence of strain rates to stress fields (Sun et al., 2017).

Finally it would be also interesting to see or at least discuss how the model results are sensitive to other uncertainties in the model; this includes the description of the bedrock and the basal friction law, especially the linear assumption that is used here.
Reply: We added these lines in Model improvements to cover this issue:
Ice thickness and basal topography with resolution of 150 m became available for main outlet glaciers of Greenland (Morlighem et al., 2017) recently (Fig. S3). This eases finer mesh resolution to be used for modeling which then might reveal more details of ice-stream behavior especially perpendicular-to-flow direction, including more precise shear-margin-weakening and calving near side walls. Our assumption of simple Weertman basal drag (Eq. 7) may be improved by implementing a physics-based basal sliding law (Schoof, 2010; Gagliardini et al., 2014; Tsai et al., 2015), although basal drag accounts for only about 2% of present-day buttressing (Shapero et al., 2016). An improved sliding relation would likely produce more speedup and retreats in model results as dynamic thinning constantly reduce the effective pressure which leads to

lower basal shear stress.

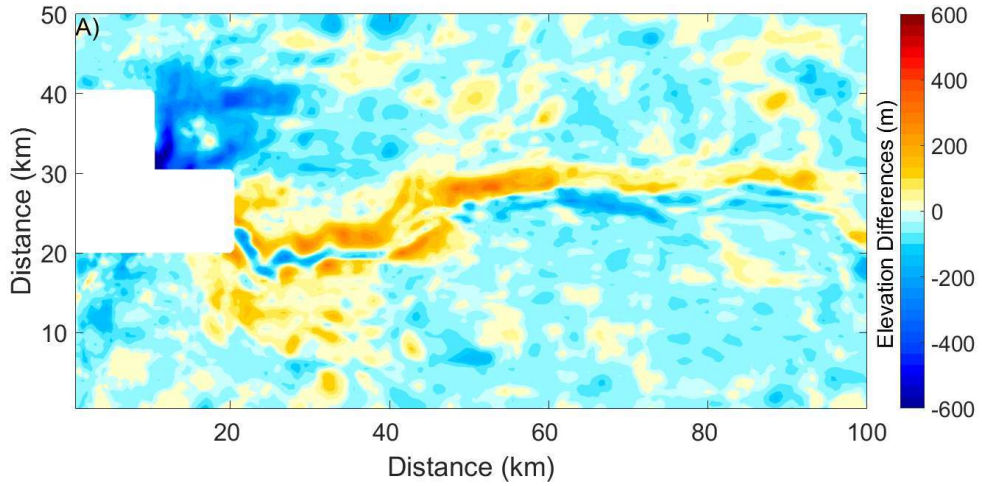

Figure S3. Bed elevation from BedMachine v3 (Morlighem et al., 2017) minus those from (Gogineni, 2012) used in this paper.

Referee #2

General Comments*: The model approach resembles previous studies by Muresan et al. 2016 by using ocean temperatures as a forcing to a dynamic ice flow model. However, Xiaoran Guo et al. expands the approach by going into more detail on seasonality and viscosity changes, while also starting their model in 2004 (not in 1990 as Muresan et al does) where they provide evidence that there is a shift in flow regime. Thus, there is a scientific advance within the field, by exploring ways to improve methods for modelling the behaviour of fast flowing ice streams. These types of model studies requires a lot of technical settings and tuning of the model which is very complicated and hard to explain in an easy-to-understand way. However, in order to satisfy the demand of traceability of results, this is the most important part of the paper. The model setup sections are not doing this sufficiently, in their current state.*

Specific comments*: Model description sections: Initialisation and calibration should be improved to make it clearer exactly what has been done. In particular I am missing information about what basal and surface geometry is used in the inversion process and also how values for basal friction and ice softness are derived. Furthermore, I am curious about the mesh resolution used in the model and in particular how this looks across the shear margins.*

Reply: Yes this is something the other referees mentioned as well, so we have extensively rewritten section 2.3.

First we added the mesh resolution and refer to a new Fig.1C from line 99:

… but the fast flow area is only around 10 km in width. We use a highest mesh resolution of 500 m that covers the whole fast-flow-area including the shear margin (Fig. 1C), while the rest of the glacier has 1000 m resolution.

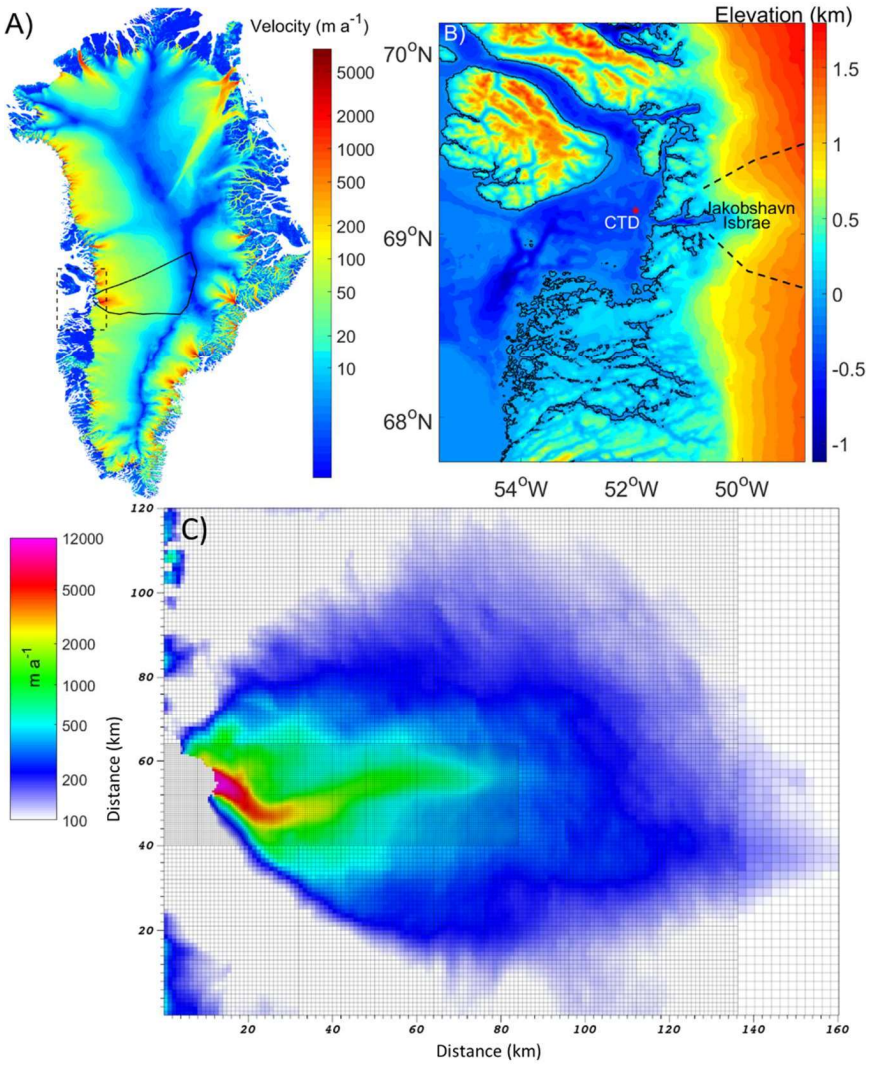

Figure 2. A) Greenland ice sheet flow speeds from Joughin et al. (2018), with the Jakobshavn drainage basin outlined by the solid black line and the area shown in panel B by the dashed box. B) Ilulissat Fjord and Disko Bay bathymetry from Jakobsson et al. (2012), with the CTD (Conductivity Temperature Depth) site used for ocean temperature here marked by the red star. C) Example of the mesh used with finest resolution of 500 m with modeled velocities at the beginning of 2004.

We change the description of the initialization procedure (line 199 onwards), to answer questions on geometry and method used for inversion.

1) We solved the inverse problem for basal conditions (Eq. 7) and stiffening factor using 2010 velocities (Joughin et al., 2010) and 2009 geometry (Gogineni et al., 2012), following Cornford et al. (2015). Our friction coefficient field is shown in Figure 3. Figure S2 shows the discrepancy between observed velocity field (Joughin et al., 2010) and the velocity derived from the inversion.

***Basal geometry**: It is not stated anywhere what basal geometry is used. As, the authors also state in the discussion, geometry is the most important factor for ice stream*

stability and thus the results of the retreating calving front should furthermore be mapped on top of a basal geometry map in 2d plan view (seen from above). The retreat pattern relation to basal geometry should be discussed in relation to other studies modelling the future behaviour of Jakobshavns Isbræ.

Reply: Our basal topography data come from (Gogineni et al., 2012). We solved the inverse problem for basal conditions (Eq. 7) and stiffening factor using 2010 velocities (Joughin et al., 2010) and 2009 geometry (Gogineni et al., 2012).

We plotted Jakobshavn's retreat in Fig. 5 in 1-d considering the convenience of comparison with previous studies (Nick et al., 2013; Muresan et al., 2016). We added a panel to Fig. 7 showing modelled front retreats along its basal trough using the best set of parameters, as requested by the referee.

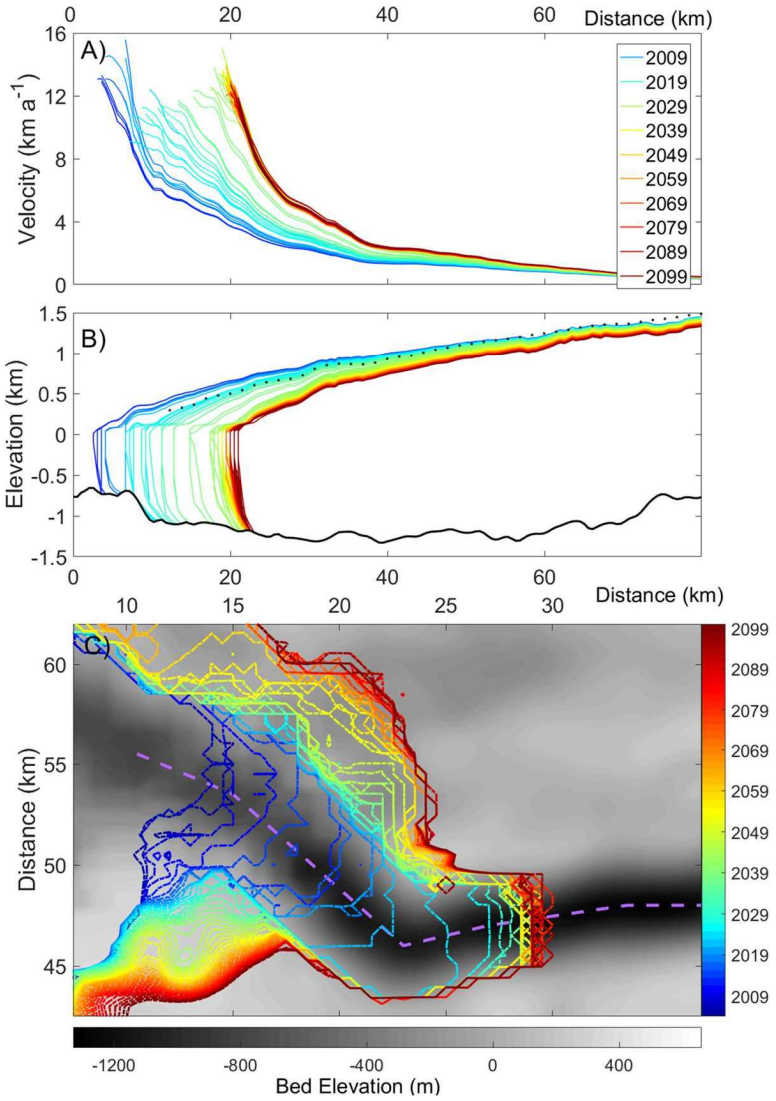

Figure 7. Modeled profiles of (A) January velocity and (B) January surface elevation along the center-flow-line (purple dash line in panel C) of Jakobshavn Isbræ from 2004 to 2099 for the RCP4.5 scenario. Bedrock elevation is shown in black. Black dotted line is the surface elevation profile extracted from radar data measured around 2010 (Gogineni et al., 2012). Profiles are shown at intervals of 1 years. Profiles are color-coded in the legend and range from blue to green and red. (C) Modeled July front positions (color bar) over its bedrock

(grayscale bar) at intervals of 2 years.

In relation to starting in 2004*: To my understanding, and also what you describe for the model, a stiff ice mélange has a butressing effect. Thus, it seems strange to me that the glacier is stable from 2004 and onwards, if it just lost an important butressing?*
Reply: Yes, our description was confusing and imprecise. The annual minimum extent of Jakobshavn retreats ~ 2 km from 2004 to 2005, but then stabilizes until 2007 (Joughin et al. 2010). Front velocities increase slowly from 2004-2007 (~5.9% a^{-1}). Annual maximum extents are stable over the 2004-2007 period. We change the text as :
The annual minimum extent of Jakobshavn retreats ~ 2 km from 2004 to 2005 following the loss of melange butressing, but then stabilizes until 2007 (Joughin et al. 2010). Front velocities increase slowly from 2004-2007 (~5.9% a^{-1}). Annual maximum extents are stable over the 2004-2007 period. This also makes 2004 a good time from which to start transient simulations.

Line by line comments*: Section 1 Generally, there is confusion about the definition of a floating ice shelf and a stiff ice mélange throughout the section.*
Reply: We cannot understand the confusion the referee mentions. We are using standard definitions: ice mélange is the broken bergs and sea ice in front of the calving front. Ice tongue and ice shelf mean the floating glacier ice that is mechanically coupled with the inland glacier.

Line 70-72*: Needs a reference*
Reply: Done:
However, in the Jakobshavn case, both Weertman and Coulomb sliding produce very similar fluxes because the basal shear stresses along the main trough are typically only 2 % of the driving force (**Shapero et al., 2016**).

Section 2 Line 102*: what basal map do you use? Line 123-124: Please refer us to a study where the method of solving the inverse problem where two unknown is discussed (or explain in detail here how that would work, and how you can trust the outcome). I think this is an important point as viscosity is non-linear.*
Reply: The method is well established in BISICLES, and described e.g. by Cornford et al. (2015). It is possible because vertically integrated shear is used rather than a full Stokes formulation as in e.g. ELMER/ice. We solved the inverse problem for basal conditions (Eq. 7) and stiffening factor using 2010 velocities (Joughin et al., 2010) and 2009 geometry (Gogineni et al., 2012), following Cornford et al. (2015).

Section 2.2*: Should just be titled Forcing (and not climate forcing*
Reply: Done. We change the title to 'Forcing'.

Line 135: What is CTD?
Reply: CTD is defined in Fig. 1 caption as "**CTD (Conductivity Temperature Depth)**".

Line 136: At what depth is the ocean temperature a good approximation?
Reply: We use 300 m depths. Cowton et al. (2018) achieved success in simulating the terminus position and yearly variability of 10 glaciers along the east coast of Greenland using mean 200-400 m depth temperatures from reanalysis data.
We use ocean temperatures at depth ~ 300 m collected from a CTD site close to the mouth of Ilulissat fjord (Fig.1) as an approximation of ocean temperatures near the glacier grounding line.

Line 153: Use alpha1 and alpha2 instead of the calibrated numbers
Reply: Equation 9 now reads: $\alpha = \alpha_1 + \alpha_2 T. (9)$

Line 157-160: MAR is used to estimate the runoff in equation 10. Later on Racmo is used as forcing. It is not clear why you use two different models, and when they are used.
Reply: Yes we clarify this after line 183 at the end of section 2.2. For the period 2004-2014, SMB and surface water run-off forcing come from MAR model outputs. Because RACMO outputs cover only the period of 2006-2099. For the period 2015-2099, our SMB and run-off forcing are from RACMO outputs. We use the overlapping period 2006-2014 to correct the bias between two models outputs.

Line 169: Make it clear that it is your model your are talking about
Reply: Here are talking about the RACMO forcing as said as the first word on line 170. Hence not from our simulation.

Line 169: Write out SMB
Reply: SMB is already defined in Line 111: where M_s, M_b are surface mass balance (SMB)…

Line 174-177: Please state in what equation this ocean forcing goes into.
Reply: Ocean temperature forcing affects mélange buttressing and sub-shelf melting (Eq. 10, 13). Ocean forcing in Equations 10 and 13 should relate to temperatures off the continental shelf close to the fjord mouth.

Section 2.3
Line 187: The dataset described here is only 2d, your model is in 3d, so I am not sure what you are using this for?
Reply: The sentence is: "Detailed bedrock topography and ice thickness data in the year 2009 come from Gogineni et al. (2012)." Bedrock topography is a 2d dataset, ice thickness is the vertical direction dataset, we use these in our 3d model. BISICLES calculates surface elevations by Eq.1.

Line 188: to my understanding, the sudden disappearance
Reply: We prefer disintegration as it cannot have simply disappeared.

Line 202: please remind us what beta is
Reply: This section has been completely rewritten see reply to line 218 below.

Line 209-210: What does similar mean? How far off are we talking here? And please state why you use the 1998 profile when the model is starting in 2004.
Reply: New Fig. S2 (see answer to line 218) shows the surface elevation profiles. We use that because the geometry in 2004 is unknown. In fact we only need the height at the grounding line, not the whole profile.

Line 214: Why is it the 8th, needs clarification.
Reply: Agreed and rephrased (line 218).

Line 217: Aha, good to know already in line 209-210
Reply: Agreed and rephrased (line 218).

Line 218-219: The glacier is definitely not in steady state in 2004, please rephrase 2.4 Model calibration. This section is very confusing to me. I think it needs a rewrite to become clearer.
Reply: Agreed. We rewrote the section 2.3:

1) We solved the inverse problem for basal conditions (Eq. 7) and stiffening factor using 2010 velocities (Joughin et al., 2010) and 2009 geometry (Gogineni et al., 2012), following Cornford et al. (2015). Our friction coefficient and stiffening factor fields are shown in Fig. 3. Fig. S1 shows the discrepancy between observed velocity field (Joughin et al., 2010) and the velocity derived from the inversion.
2) Starting from the inversion of step 1, we let the model glacier evolve freely without calving and with zero SMB and with sub-shelf melting (γ=0.0238) forced by repeating the observed 2004 ocean temperature for 11 years until its surface elevation profile reached a state shown in Fig. S2.
3) We carried out several 10-year simulations each with different β values estimated. These simulations were forced by repeatedly applying the 2004 seasonal climate forcing so that the glacier approaches a steady state. From these, we selected the β that provided a calving front position closest to that observed in 2004. The best β here is 0.034. This is our best guess for the 2004 state. The annual minimum extent of Jakobshavn retreats ~ 2 km from 2004 to 2005 following the loss of melange butressing, but then stabilizes until 2007 (Joughin et al. 2010). Annual maximum extents are stable over the 2004-2007 period. Front velocities increase slowly from 2004-2007 (~5.9% a^{-1} Joughin et al. 2010), and the model simulated velocities increase by about 3% a^{-1}. This period of relative stability also makes 2004 a good time from which to start transient simulations.

Basal friction coefficient values downstream of the 2010 grounding line were set equal to that in the nearest 2010 grounded location. This was necessary because steps 2 and 3 involved grounding line advance beyond the region for which basal friction coefficients had been inferred. The geometry after this spin up procedure, and the

friction coefficient and stiffening factor distribution from the inversion in step 1 were used as the initial condition for model calibration.

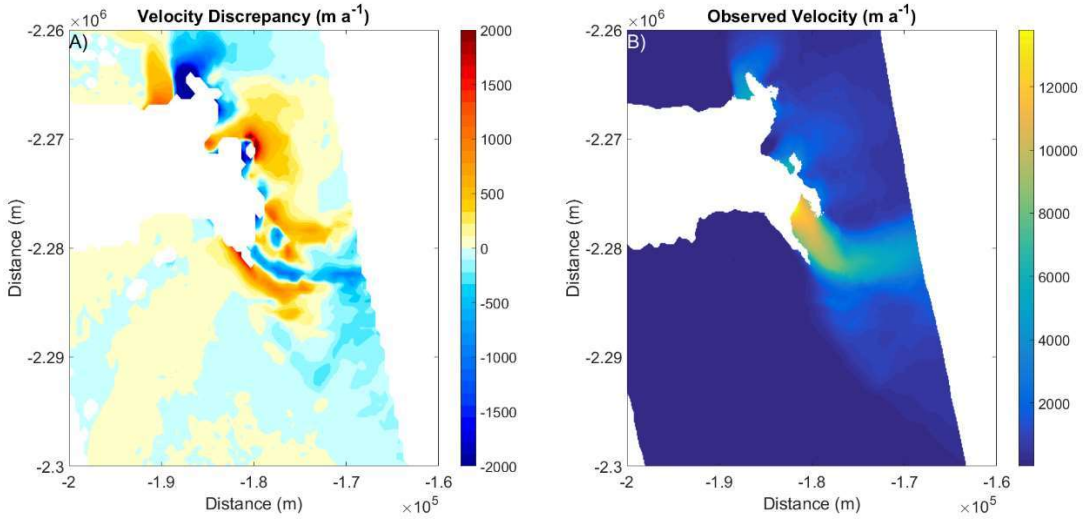

Figure S1. A) Velocity discrepancy (velocity from inversion - observed) and B) the observed velocity field (Joughin et al., 2010).

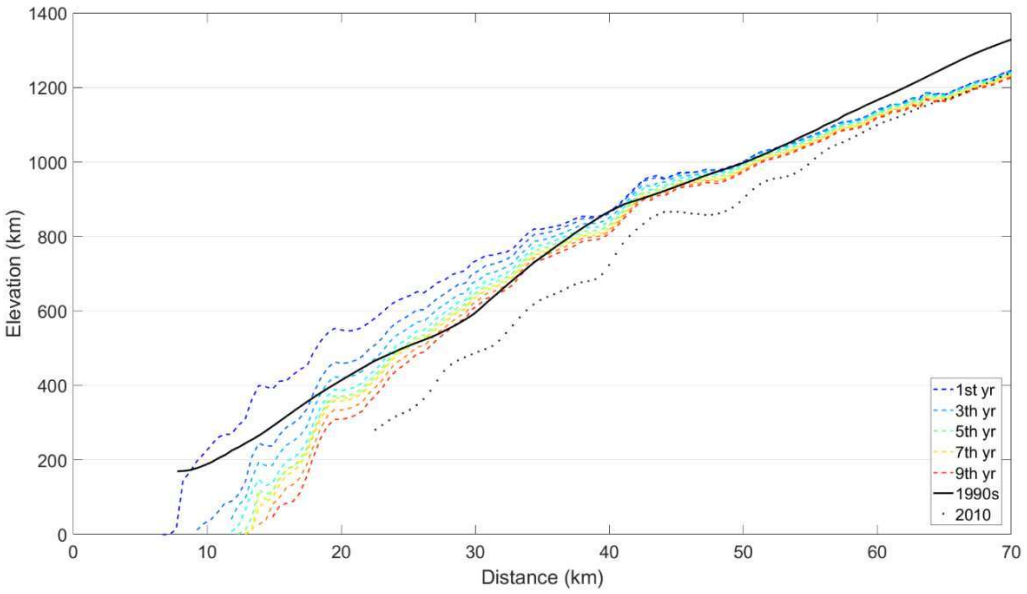

Figure S2. Profiles of surface elevation during the initialization procedure (section 2.3) step 3. Black solid line and black dashed line show the known profiles taken in the 1990s (Bamber et al., 2001) and 2010 (Gogineni et al., 2012) respectively. The profile with legend '1st yr' is the final state of section 2.3 step 2. The profile '7th yr' is the geometry rebuilt for 2004's Jakobshavn, which is the initial state for later simulations.

Line 235*: rephrase sentence Line 235-245: I am confused about this whole paragraph. The following paragraph (Line 246-259) is better structured, could this perhaps be the start of the section?*

Reply: We prefer to discuss optimal parameter values and then sensitivities, so we rewrite the paragraph:

The parameters in the model, α, β and γ representing mélange buttressing, crevasse depth sensitivity to surface runoff, and shelf melt sensitivity to ocean temperatures need to be estimated. The measured relationship between ocean temperatures and sub-shelf melt rate (Motyka et al., 2011) gives the value of γ to be 0.238. We tune parameters α and β manually to best reproduce Jakobshavn Isbræ's calving front position and surface velocity evolution for the 10 year period 2004-2013. Reproducing the total retreat distance and the temporary stable state after 2012 were secondary desirable features to match. The best set of parameters are α_1=0.82, α_2=0.111, β=0.0638. Since these values come from a manual search we do not claim them to be the best in all parameter space. We assess model sensitivity to the parameter values next.

Line 274-284*: This whole paragraph needs clarification*
Reply: This paragraph (Line 274-284) has been rewritten:
The two biggest mismatches occur with the 2007 and especially 2013 velocities (Fig. 5). 2013 has the lowest simulated surface water run-off (Fig. 2) of all the years since 2004. The Benn calving model we use is sensitive to runoff, with reduced run-off leading to lower crevasse-penetration-depth and reduced terminus fracturing thus increasing its buttressing force. Furthermore 2013 had relatively cool ocean temperatures which were lower than the average of 2004-2013. The cool ocean temperatures also increased buttressing, leading to low simulated annual mean velocities. Jakobshavn Isbræ did not in fact slow down very much in 2013 because there were calving events that are unrepresented in our model. The relevant mechanisms are discussed later.

Figure 5A*: How is the calving front retreat defined? Is it just a comparison at points along a centre flow line? And it this representative of the general retreat?*
Reply: Yes, it is defined as the distance along the center-flow-line. See Fig. 7 caption.

Section 3 Figure 7*: I would be more interested in seeing the retreat from above, the center flowline bedmap does not explain the stop of retreat.*
Reply: Agreed. We add a new panel to Fig. 7 showing the 2-d map and new figs 8 and 9 showing more details that help explain the retreat cessation.
Examination of the change in velocities during the simulation (Fig. 9) suggests that the explanation for this stability is strong flow convergence near the future glacier front that largely offsets dynamic thinning. Notice that the South side of the fast-flow-area in 20th century was quite close to ice-free land, while in later half of this century convergent flow in the South is fed by a substantial area of ice stream.

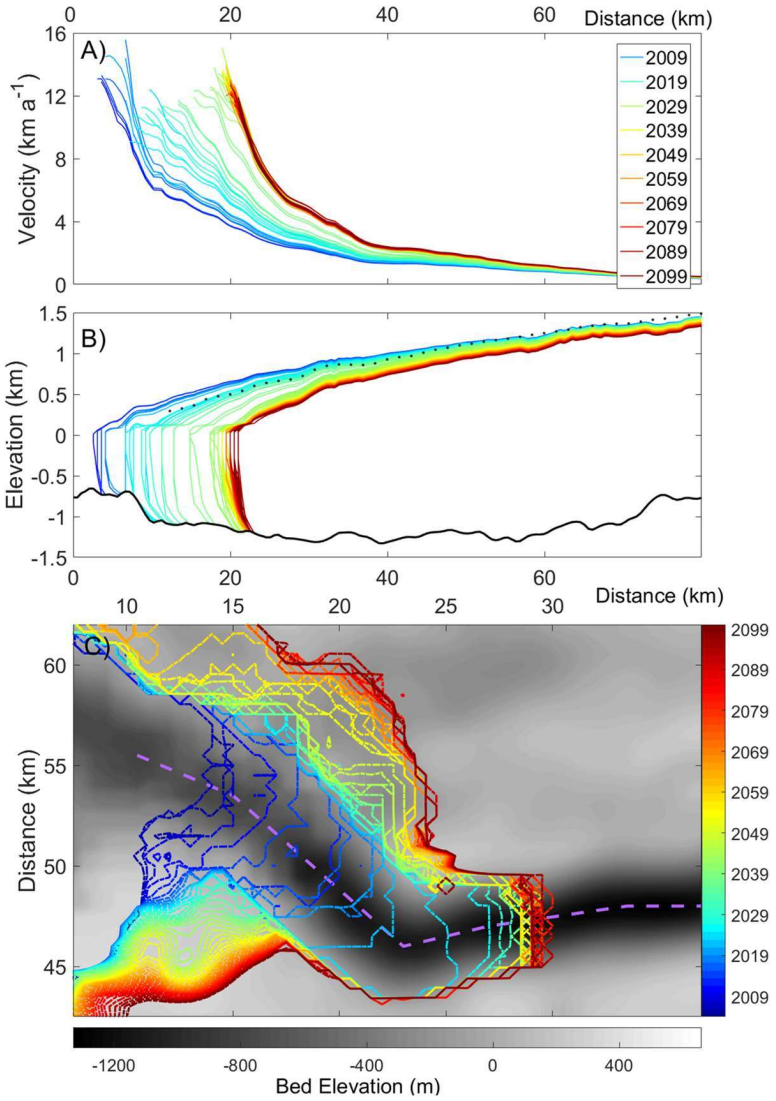

Figure 7. Modeled profiles of (A) January velocity and (B) January surface elevation along the center-flow-line (purple dash line in panel C) of Jakobshavn Isbræ from 2004 to 2099 for the RCP4.5 scenario. Bedrock elevation is shown in black. Black dotted line is the surface elevation profile extracted from radar data measured around 2010 (Gogineni et al., 2012). Profiles are shown at intervals of 1 years. Profiles are color-coded in the legend and range from blue to green and red. (C) Modeled July front positions (color bar) over its bedrock (grayscale bar) at intervals of 2 years.

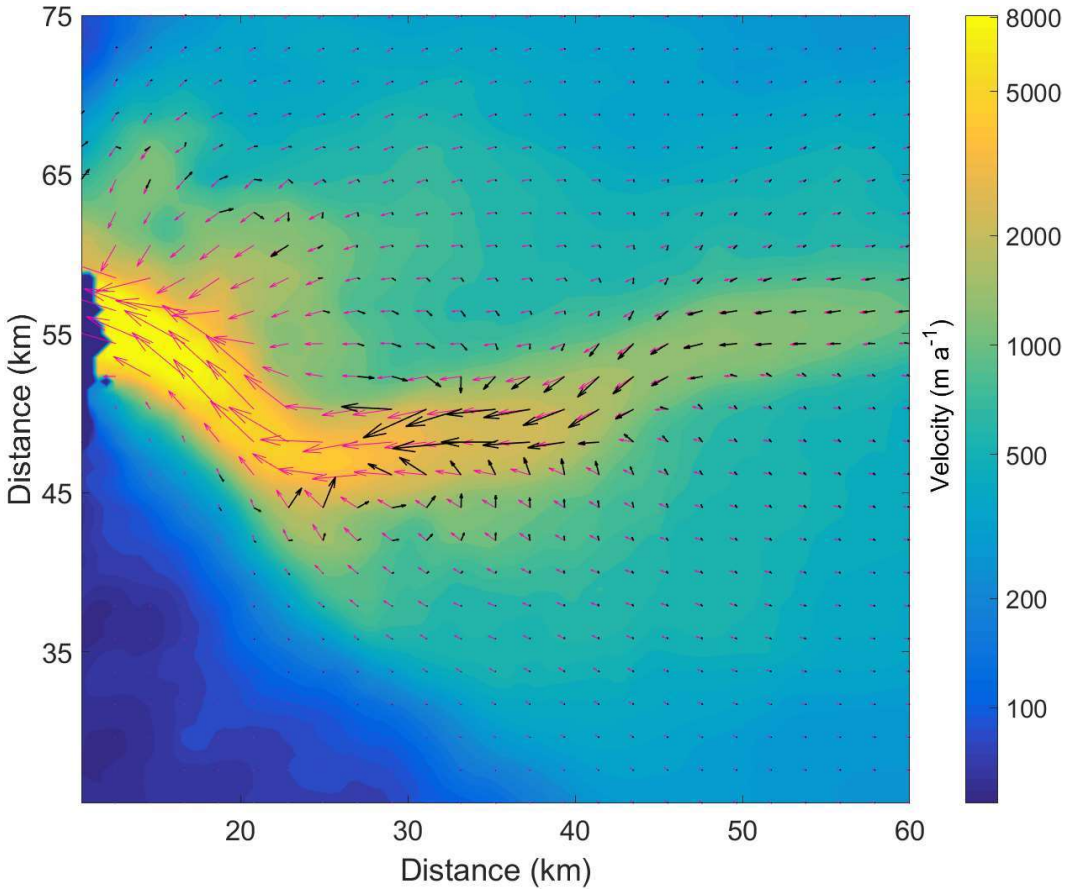

Figure 9. Simulated velocity vectors in 2004 (pink vectors) with their magnitudes (right color bar) and velocity difference between 2004 and 2099 (2099's minus 2004's, black vectors), for clarity vector lengths are clipped at 5 km a^{-1}.

Line 322*: Make it clear that you are talking about you model version of Jakobshavn Isbræ.*

Reply: OK: In our modelled results under this forcing, Jakobshavn Isbræ continues its retreat (Fig. 7) for 18 years after 2013, producing a total grounding line retreat of ~18 km upstream.

Section 4: *It confused me a bit that you called this Discussion as a lot of important results are also presented here.*

Reply: Our modelled seasonal cycle of shear margin weakening is the main distinguishable feature comparing with previous studies. So it is convenient to put results, such as viscosity changes, here to make comparison with others.

Line 370-372*: This sentence does not make sense to me, does freshly calved ice bergs really provide any resistance?*

Reply: Agreed. We deleted this sentence.

Line: 376-377*: here you call it a stiff ice mélange, I think you should use this term throughout, especially in the intro.*

Reply: We are using standard definitions: ice mélange is the broken bergs and sea ice in front of the calving front. Ice tongue and ice shelf mean the floating glacier ice that is mechanically coupled with the inland glacier.

Section 4.2 *I am a bit confused, are the results of changes in the effective viscosity shown in figure 8 results from your forward run? And if so, how does the fact that you are keeping ice softness constant influence these results? I think there must be an effect in the softening from the thermodynamics as well?*
Reply: Yes. Fig. 10 (old fig. 8) shows results from the forward run. We plotted $\Phi\mu$ (Eq. 5) in Fig. 10. Our Ice stiffness factor Φ is fixed but ice viscosity μ varies in time. Bondzio et al., 2017 used a thermomechanical ice flow model to evolve the ice viscosity, which depends on a damage parameter that soften the ice in the shear margins. But their damage parameter also stays constant in time. Thus both our and their models only consider the contribution from strain rate weakening in time to evolving viscosity. Thermodynamics could play some role in changing viscosity, presumably if the ice temperatures increased over time. We suppose that this would be a minor effect compared with mechanical softening, and the temperature of the ice is fixed in our model.

Section 4.3 *Good to have comparisons with previous results, I think a key point, which you focus very little on, is that the retreat stops in the same area in all the studies (if I understood this correctly)? I think that if you also add figures showing basal geometry and retreat as suggested earlier, this point is easily added.*
Reply: In previous studies, Nick et al. (2013) and Muresan et al. (2016) didn't reproduce Jakobshavn's retreats to the bottom of its over-deepened basin, which we did (Fig. 5). We added the 2-d views of the past and predicted front retreats to Fig. 7C and Fig. 8. In our range of future projections we find retreat is slowed in the same places and new Fig. 9 tries to explain the reason for the retreat stoppage.

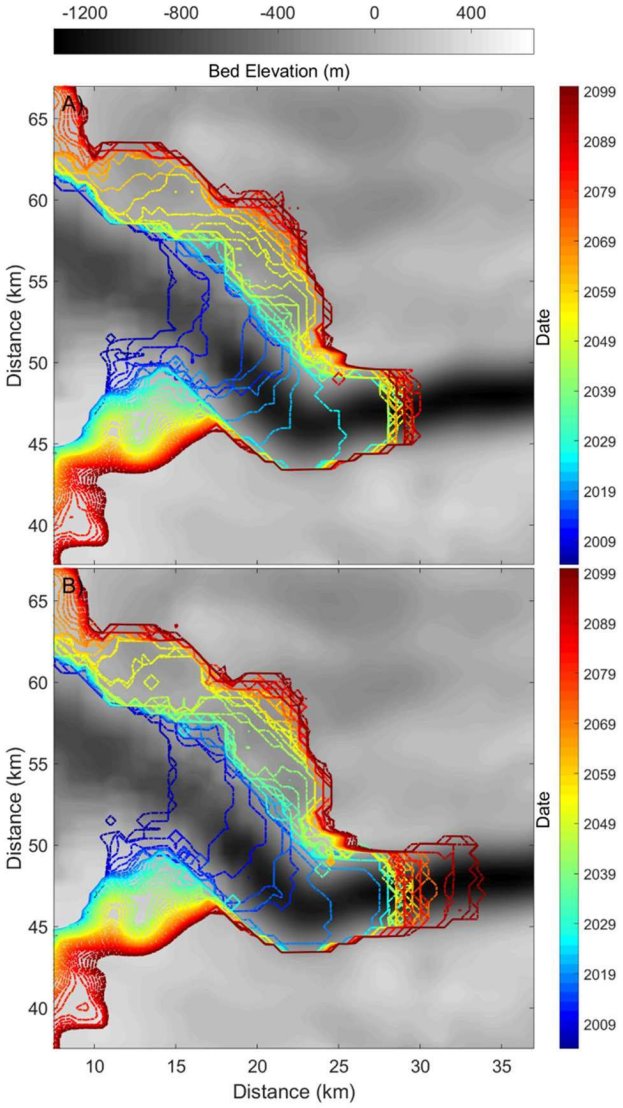

Figure 8. Upper and lower estimates of July front positions within this century with colors indicating the date (color bar) for A) lower bound with scalings of (1,0.8) and the HadGEM-ES forcing B) upper bound of mass loss projection with (α, γ) parameter scalings of (1.2,1), and the 7-model ensemble climate forcing.

***Line 498-499**: What do you mean by two-dimensional ice flow patterns?*

Reply: Here 'ice flow patterns' refers to 'ice velocity and viscosity structures'. Thus:

We successfully model two-dimensional ice velocity and viscosity structures and their seasonal variations for Jakobshavn Isbræ, which are missing from several previous modeling studies. Moreover, capturing these two-dimensional structures allows us to handle the influence of horizontal velocity shear on effective ice viscosity, which impacts on speedup processes of Jakobshavn Isbræ.

Anonymous Referee #3

1 Summary statement

The manuscript "Simulated retreat of Jakobshavn Isbrae during the 21st century" by X. Guo and colleagues presents results on the simulation of Jakobshavn Isbrae over the 21st century, calibrated to match its current configuration and recent evolution. The model includes buttressing provided by the ice melange and a calving law based on crevasse-depth, and the forcings are based on Global Climate Models (GCMs). The results suggest that the glacier will continue to retreat and lose mass during the 21st century, reaching 5.6 mm of sea level equivalent by the end of the century.

The paper is well written, usually easy to follow (except for the initialization procedure that is quite complicated), and the figures appropriate. However, some additional explanations are needed to understand the choices made for the calibration of several parameters, for some of the datasets used, or for the initialization procedure. Furthermore, only a couple of figures show the evolution of the glacier over a flow line for one given simulation of the ensemble. It would be valuable to show the spread of the model results for the different parameters used and the different forcings, but also to show the spatial evolution of the ice front not just on a flow line but for the entire basin. Finally, the authors mention that the calving law based on crevasse-depth prevents the calving of the glacier once the thickness becomes too large. This is the contrary of what is physically expected: a tall cliff with a large height above sea level leads to more calving, so there is no reason for the calving to get reduced towards the end of the simulations.

2 Major comments

The bedrock and bathymetry used come from Jakobsson et al. (2012) and Gogineni et al. (2012), while the newer bedrock elevation maps of Greenland typically used in ice sheet modeling are Bamber et al. (2013) and Morlighem et al. (2017), so it is a rather interesting choice. There are probably good reasons for using these maps, but they are not well explained. It would be good quantify the impact of this choice on the simulations compared to other choices, or at least explain the differences expected.

Reply: Our glacier geometry data (Gogineni et al., 2012) is derived from the same institution's products as used in BedMachine V3 with data processed by the Center for Remote Sensing of Ice Sheets (CReSIS, Leuschenetal., 2010 updated 2016). For computing resource considerations, we chose the earlier product because it has 500-meter-resolution. The difference between these two bedrock elevations are shown in Fig. S3.

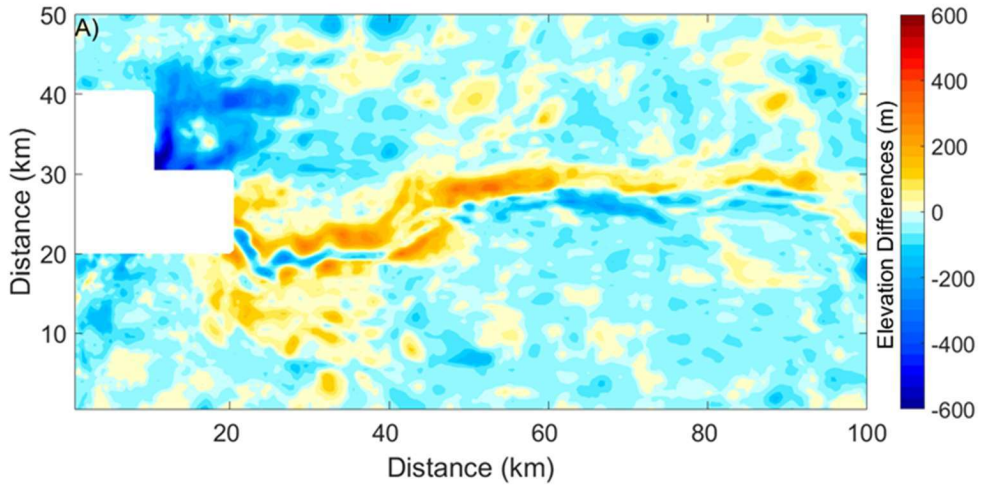

Figure S3. A) Bed elevation from BedMachine v3 (Morlighem et al., 2017) minus those from (Gogineni, 2012) used in this paper.

The calving law is based on crevasse-depth based calving only, so that calving happens when deep surface crevasses develop in the presence of surface water. Is this representation of calving sufficient to represent the different types of calving throughout the year and as the glacier retreats to deeper grounds? It seems that the model is not able to simulate calving in winter that is becoming important towards the end of the simulation. Would a different parameterization of calving lead to different results? This is a rather important question as it contradicts the marine ice cliff instability that predicts faster and faster retreat as glaciers retreat to deeper grounds and the ice thickness increases. So what is the impact of choosing a crevasse-depth based calving? This should be addressed in more details in the discussion.

Reply: As we state in our paper at quite some length, our model clearly does not represent winter calving, which does become more important later in observational record. This is beyond dispute.

Winter calving is poorly understood. Its mechanism could be non-hydrostatic processes including the terminus uplifting due to super-buoyant condition with the opening of basal crevasses (James et al, 2014; Xie et al., 2016; Benn et al., 2017), which is beyond the capability of our model. This means that other extensions of calving parameterizations are needed. But this is not particularly relevant to the MICI mechanism in our opinion. We add this text:

Winter calving can occur in later winter (Cassotto et al., 2015) when calving front height is at its annual minimum and presumably at its least vulnerable to structural failure. Hence, MICI (Marine Ice Cliff Instability) cannot explain this type of calving, and winter calving is specifically excluded from parametrizations of MICI (Pollard et

al., 2018). The existence of winter calving has greatly reduced the range of seasonal fluctuations in front position, which inhibited the growing of a temporary ice shelf that would buttress the grounded ice. Thus, lack of winter calving would cause underestimation of dynamic thinning as the glacier grows in winter.

Our calving criterion does not predict lower calving rates as the glacier retreats into its over-deepened basin. Although calving front height keep increasing during retreats, dynamic thinning rises highly non-linearly along with it, which leads to formation of a thin shelf which is then vulnerable to calving.

Our modeled retreats are not in contradiction to MISI (Marine Ice Shelf Instability). Most of the glacier buttressing is from the lateral margins and not the bed, this means that e.g. the advance of the glacier in 2018 due to ocean cooling does not contradict the MISI either since the calving position is not only governed by bed geometry. The cessation of retreat during the later part of our ~ 60 year simulation can be attributed to the strong flow convergence near the glacier front that largely offsets the dynamic thinning (Fig. 9). Notice that the south side of the fast-flow-area in last century is quite close to ice-free land while in later half of this century convergent flow in the south is fed by a substantial area of ice stream. We add this point to the text. We discuss all these features of calving in section 4.

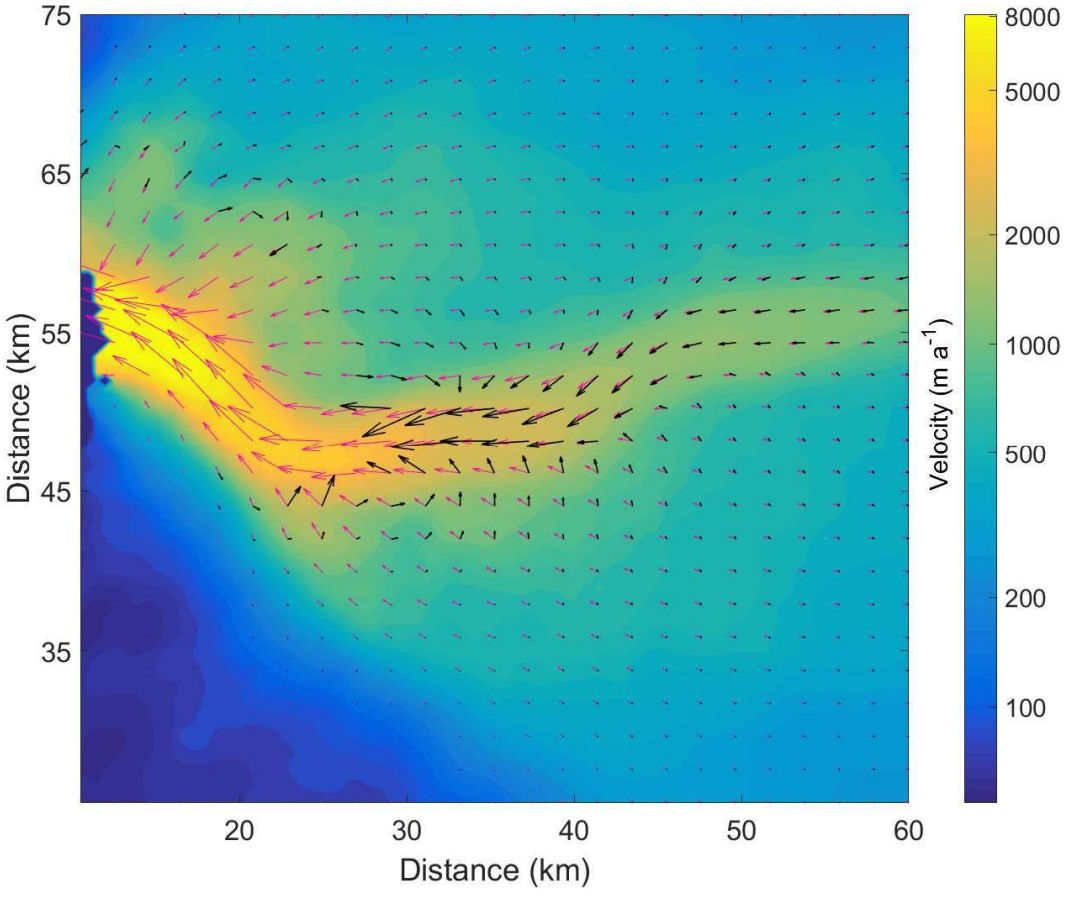

Figure 9. Simulated velocity vectors in 2004 (pink vectors) with their magnitudes (right color bar)

and velocity difference between 2004 and 2099 (2099's minus 2004's, black vectors), for clarity vector lengths are clipped at 5 km a^{-1}.

The role of melange and its parameterization are said to have a relatively large impact on the results, but the exact role of melange and the associated processes that could impact calving remains unclear. What happens to the simulations when the buttressing provided by the ice melange is removed?

Reply: Ice mélange buttressing effects played a decisive role in the recent retreating and evolving of Jakobshavn (Joughin et al., 2004; Joughin et al., 2008; Vieli et al., 2011; Nick et al., 2013). In our model, mélange buttressing does affect calving by altering the stress field that contributes to crevasse penetration depth (Eq. 12), with the sensitivity of the corresponded parameter α tested (Section 2.4). This paper aims at reproducing the evolutions of Jakobshavn in the real world where mélange buttressing matters, for example we add: Our buttressing parameterization gives a longitudinal resistance that is 18% of the driving force at calving front (Eq. 10), for the instance of 2004.

The processes included in the simulations include many parameters, and these parameters are not always justified or explained. In particular what they physically represent and what the impact is for the simulations. For example: How much buttressing does the melange represent? What is the equivalent ice thickness needed to get a similar buttressing? What is the tuning scalar for the run-off in the crevasses? What ocean temperatures are used for the forcing, and how was this choice made? How are the ocean temperature converted from the far field, to the fjord and to the grounding line region?

Reply: We explain our parameterization for external forcing into fine details in section 2.2. The verifications of our parameterizations are shown in Fig. 5 and discussed in section 4. We give additional details on various questions the referee raises:

Our buttressing parameterization gives a longitudinal resistance that is 18% of the driving force at calving front (Eq. 10), for the instance of 2004.

We tune parameters α (over the range 0.7−1.2 for α_1 and 0.09-0.12 for α_2) and β (0.04 - 0.075) manually.

Local ocean circulation in Ilulissat fjord driven by buoyancy plume brings deep water from outside to the grounding line of Jakobshavn, and renews the fjord within 90 days in summer (Gladish et al., 2015). Generally, Jakobshavn's fjord is ~ 800 m deep but with a sill of only ~ 200 m depth at its entrance. The deepest water outside the sill can flow over the sill and reach the grounding line of

Jakobshavn (Gladish et al., 2015). We use 300 m depth ocean temperatures collected from a CTD site close to the mouth of Ilulissat fjord (Fig. 1) as an approximation of ocean temperatures near the glacier grounding line. A comprehensive study focusing on ocean circulation within Ilulissat fjord validated this approximation (Gladish et al. 2015).

T_f is the far field ocean forcing temperature, taken in Disko Bay (CTD in Fig. 1), relative to pressure melting temperature under the ice shelf. Thus T and T_f are related simply by ice depth and salinity.

The initialization is rather confusing, with a target date of 2004 at the beginning of the simulations, but other datasets with different times are used for the inverse problem (2012) and the relaxed surface elevation (1998). This part should be clarified to better understand the rationale behind the initialization procedure.

Reply: Agreed, the statement was imprecise. We have rewritten this in response to other criticism on the method:

1) We solved the inverse problem for basal conditions (Eq. 7) and stiffening factor using 2010 velocities (Joughin et al., 2010) and 2009 geometry (Gogineni et al., 2012), following Cornford et al. (2015). Our friction coefficient and stiffening factor fields are shown in Fig. 3. Fig. S1 shows the discrepancy between observed velocity field (Joughin et al., 2010) and the velocity derived from the inversion.
2) Starting from the inversion of step 1, we let the model glacier evolve freely without calving and with zero SMB and with sub-shelf melting (γ=0.0238) forced by repeating the observed 2004 ocean temperature for 11 years until its surface elevation profile reached a state shown in Fig. S2.
3) We carried out several 10-year simulations each with different β values estimated. These simulations were forced by repeatedly applying the 2004 seasonal climate forcing so that the glacier approaches a steady state. From these, we selected the β that provided a calving front position closest to that observed in 2004. The best β here is 0.034. This is our best guess for the 2004 state. The annual minimum extent of Jakobshavn retreats ~ 2 km from 2004 to 2005 following the loss of melange butressing, but then stabilizes until 2007 (Joughin et al. 2010). Annual maximum extents are stable over the 2004-2007 period. Front velocities increase slowly from 2004-2007 (~5.9% a^{-1} Joughin et al. 2010), and the model simulated velocities increase by about 3% a^{-1}. This period of relative stability also makes 2004 a good time from which to start transient simulations.

Basal friction coefficient values downstream of the 2010 grounding line were set equal to that in the nearest 2010 grounded location. This was necessary because steps 2 and 3 involved grounding line advance beyond the region for which basal friction coefficients had been inferred. The geometry after this spin up procedure, and the friction coefficient and stiffening factor distribution from the inversion in step 1 were used as the initial condition for model calibration.

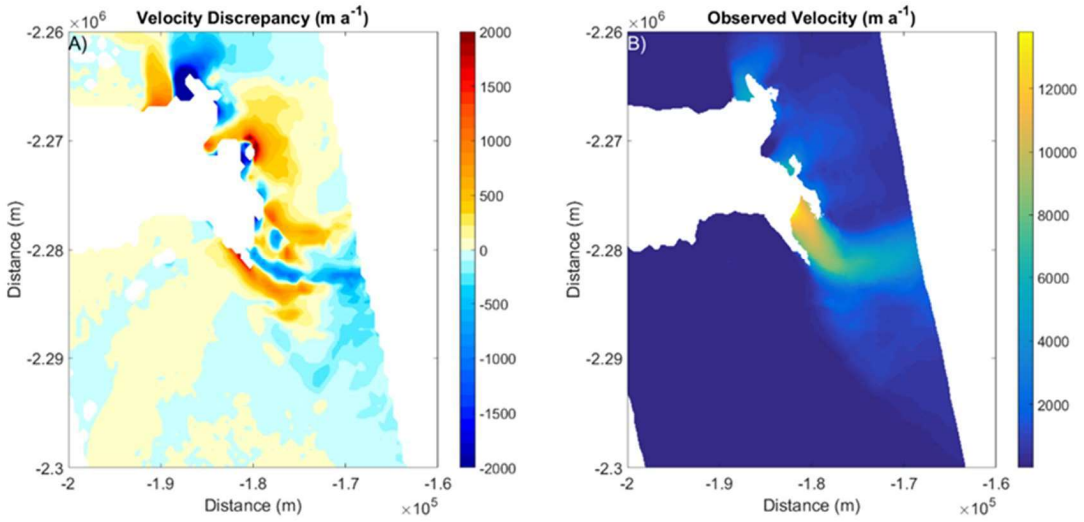

Figure S1. A) Velocity discrepancy (velocity from inversion - observed) and B) the observed velocity field (Joughin et al., 2010).

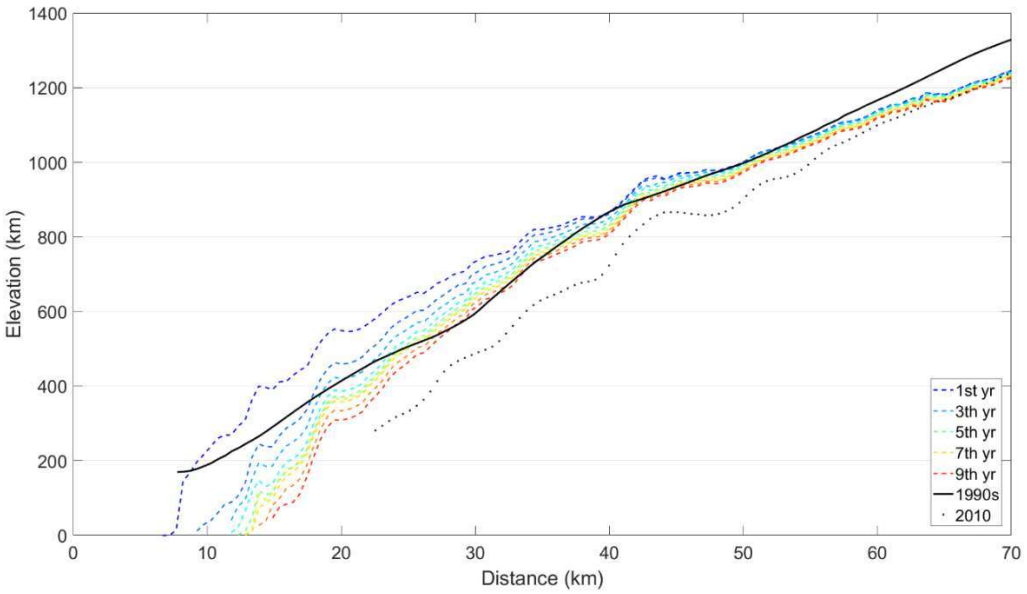

Figure S2. Profiles of surface elevation during the initialization procedure (section 2.3) step 3. Black solid line and black dashed line show the known profiles taken in the 1990s (Bamber et al., 2001) and 2010 (Gogineni et al., 2012) respectively. The profile with legend '1st yr' is the final state of section 2.3 step 2. The profile '7th yr' is the geometry rebuilt for 2004's Jakobshavn, which is the initial state for later simulations.

I am wondering how reliable the GCMs are to reproduce the temporal patterns of variability of the glacier: to my knowledge, GCMs do not get the right timing for the variability, so maybe some reanalysis data would perform better for that.

Reply: In model calibration, our forcing data comes from observations and MAR regional surface mass and energy balance model (Alexander et al. 2016) driven by the ERA-Interim reanalysis (Dee et al., 2011). The ERA-Interim reanalysis is widely used on Greenland by e.g. MAR and RACMO communities and is free of artifacts. Hence

we do not reply on ESM (GCM) data for the historical variation prior to 2014.

Finally, there are not many figures showing the results, e.g., the spatial distribution of ice front position at the end of the simulations for the different cases or the mass loss for the different cases (just a few numbers in the table). It would be a good addition to the paper to add a few figures to get a better sense of how this glacier could change in the future, such as the spread of results, the spatial evolution of the ice front, or the evolution of mass loss and discharge with time.

Reply: Agreed. We add Fig. 7c and Fig. 8 to show Jakobshavn's retreats on 2-D plane view under the forcing for best guess, lower and upper bounds of mass loss projection.

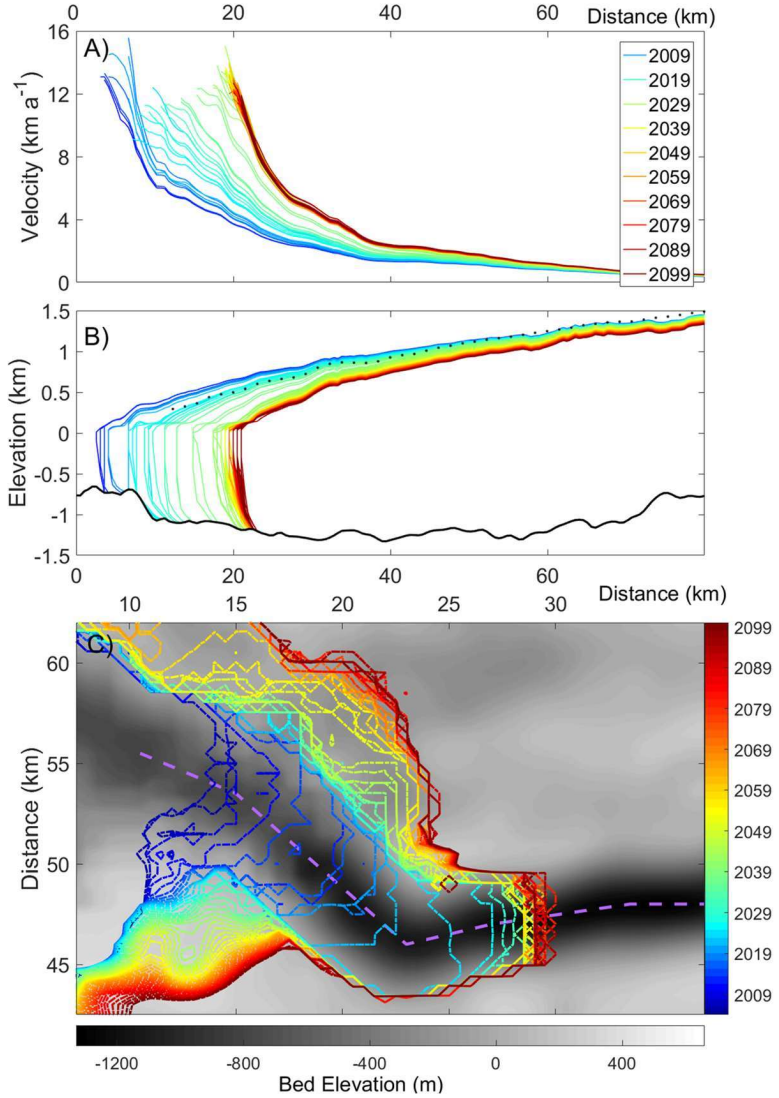

Figure 7. Modeled profiles of (A) January velocity and (B) January surface elevation along the center-flow-line (purple dash line in panel C) of Jakobshavn Isbræ from 2004 to 2099 for the RCP4.5 scenario. Bedrock elevation is shown in black. Black dotted line is the surface elevation profile extracted from radar data measured around 2010 (Gogineni et al., 2012). Profiles are shown at intervals of 1 years. Profiles are color-coded in the legend and range from blue to green and red. (C) Modeled July front positions (color bar) over its bedrock (grayscale bar) at intervals of 2 years.

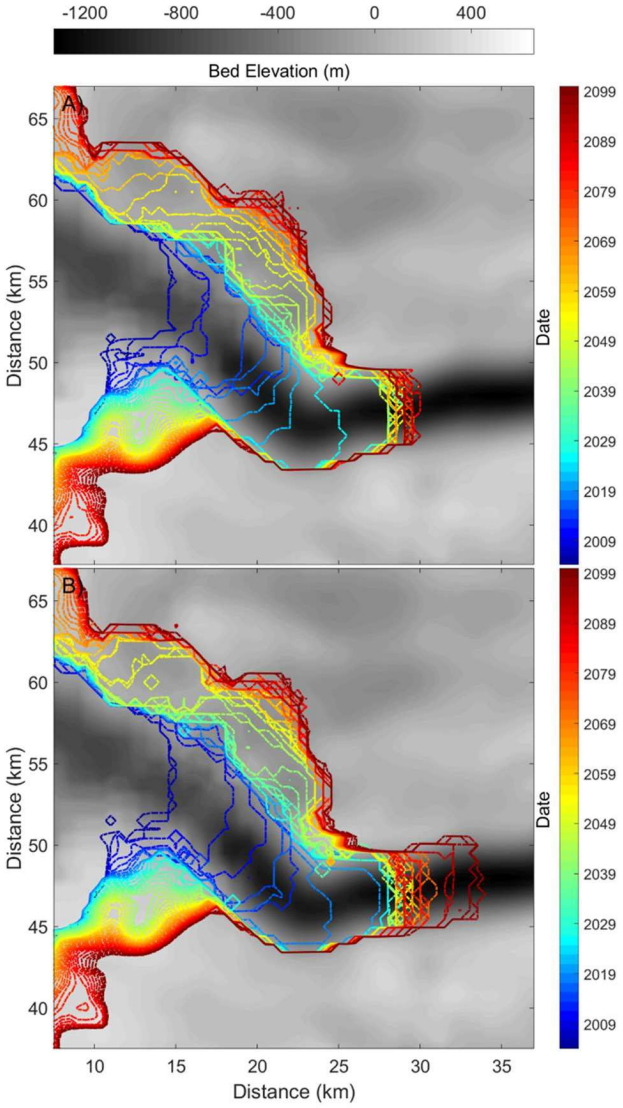

Figure 8. Upper and lower estimates of July front positions within this century with colors indicating the date (color bar) for A) lower bound with scalings of (1,0.8) and the HadGEM-ES forcing B) upper bound of mass loss projection with (α, γ) parameter scalings of (1.2,1), and the 7-model ensemble climate forcing.

3 Specific comments

p.2 l.26: "with" → "leading to a"

Reply: Done.

p.2 l.26: "5.6 mm sea-level-rise" → "5.6 mm of sea level rise"

Reply: Done.

p.2 l.28: Why is the model unable to reproduce the winter calving? Is that a limitation of the model parameterization, the representation of calving (maybe the crevasse-depth calving is just one mode of calving and does not cover all the cases), the initial conditions? And what do you think are the consequences of the lack of winter calving?

Reply: In our calving criterion, crevasse penetration depth depends on surface water run-off which equals to zero in winter, thus no calving occurs in simulation. As discussed in section 4.4, these winter calving might be the consequences of non-hydrostatic processes related to the opening of basal crevasses. The existence of winter calving has greatly reduced the range of seasonal fluctuations in front position, which inhibited the growing of a temporary ice shelf that would buttress the grounded ice. Thus, lack of winter calving would cause underestimation of dynamic thinning as the glacier grows in winter. We added some more text on this.

Winter calving can occur in later winter (Cassotto et al., 2015) when calving front height is at its annual minimum and presumably at its least vulnerable to structural failure. Hence, MICI (Marine Ice Cliff Instability) cannot explain this type of calving, and winter calving is specifically excluded from parametrizations of MICI (Pollard et al., 2018). The existence of winter calving has greatly reduced the range of seasonal fluctuations in front position, which inhibited the growing of a temporary ice shelf that would buttress the grounded ice. Thus, lack of winter calving would cause underestimation of dynamic thinning as the glacier grows in winter.

p.2 Fig.1 caption: as mentioned above, using Jakobsson et al. (2012) is a rather un-expected choice, so it would be good to justify it and quantify the difference in bedrock elevation between this map and the other more standard maps.

Reply: You may notice that Jakobsson et al. (2012) provides ocean bathymetry data (sea floor elevation). Our glacier geometry data (Gogineni et al., 2012) is derived from the same institution's products as used in BedMachine V3 with data processed by the Center for Remote Sensing of Ice Sheets (CReSIS, Leuschenetal., 2010 updated 2016). For computing resource considerations, we chose the earlier product because it has 500-meter-resolution. The differences between these two datasets are shown in Fig. S3.

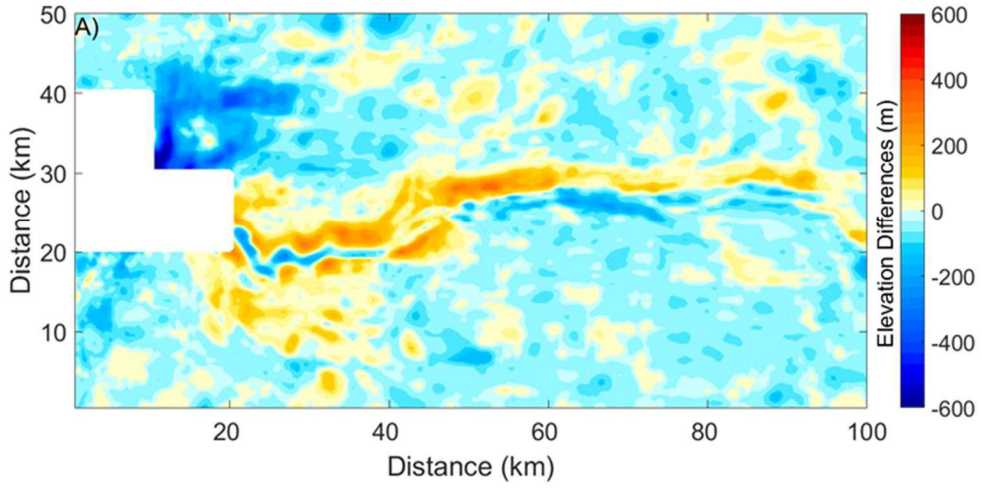

Figure S3. A) Bed elevation from BedMachine v3 (Morlighem et al., 2017) minus those from (Gogineni, 2012) used in this paper.

p.2 l.30: the 17km/a speed is a seasonal speed happening over a few months in summer and not an annual velocity, it would be good to mention that.
Reply: Yes, we modify the sentence to say:
Jakobshavn Isbræ (Fig. 1) is Greenland's largest and fastest outlet glacier, with transient speeds of up to 17 km a^{-1} (Joughin et al., 2014).

p.3 l.44: "possessed" → "had"
Reply: Done.

p.3 l.57: "far faster" → "much faster"
Reply: Done.

p.4 l.64: "must be zero at the grounding line as it begins to float": I would rather say that it is zero under the floating tongue.
Reply: Agreed. We change it to say: … it is zero at the grounding line as it begins to float.

p.4 l.74: the melange does not really belong to the ice shelf or the glacier ("its floating melange"). I am also surprised to see "desintegration" associated to "melange" because the melange changes a lot seasonally, which is rather common, so I don't understand why these changes would be qualified of desintegration.
Reply: We modify the sentence to say:
Loss of buttressing from the weakening mélange or enhanced submarine melting could have triggered the dramatic changes seen in Jakobshavn Isbræ at the end of the 20th century.

p.4 l.80: There is also a new study on Jakobshavn by Bondzio et al. (2018) using a2d plan view model and a different calving parameterization, so it would be good to include these results in the comparison.
Reply: At the end of this paragraph we added:
Bondzio et al. (2018) applied a similar calving model that remove any ice where tensile stress exceeds a threshold, as simulated with a SSA (Shallow Shelf Approximation) model, regardless of ice thickness. To represent seasonal fluctuation of front positon, their stress threshold is a stepwise constant function in time with low values in summer. After calibration, their model can closely reproduce the observed behavior from 1985 to 2018 when forced only with ocean temperatures.

p.5 l.92: "BISICLES continuum ice sheet dynamics model" → "BISICLES ice sheet model"
Reply: Done.

p.5 l.100: "in hydrostatic equilibrium": the floating part only is in equilibrium"
Reply: In BISICLES, the whole ice is in hydrostatic equilibrium (Cornford et al., 2013).

p.6 l.107: "an approximate stress balance equation": replace by the name of the approximation and a reference as they are many difference approximations of the stress balance equations

Reply: We modify this line to say:

An approximate stress balance equation (Schoof and Hindmarsh, 2010).

p.8 l.136-137: How do you use the ocean conditions outside of the fjord to constrain the conditions inside the fjord and close to the grounding line?

Reply: We add this sentence to the text:

Local ocean circulation in Ilulissat fjord driven by buoyancy plume brings deep water from outside to the grounding line of Jakobshavn, and renews the fjord within 90 days in summer (Gladish et al., 2015).

p.8 l.140: "working hypothesis": there is not much in the discussion addressing this hypothesis and whether it was a valid one.

Reply: We found good correlation between ocean temperatures on the ice-ocean interface and velocities of ice front (Fig 2). We further discuss its validation in section 4.1.

p.8 l.148: calving has been shown to be the main driver of the velocity Bondzio et al. (2017), so that changes in calving front positions could explain most of the dynamic changes of Jakobshavn Isbrae over the past three decades, so that changes in basal conditions indeed have a small impact for this glacier.

Reply: Agreed. Our basal drag coefficient is fixed in time.

p.8 l.149-150: This is an interesting way to change the buttressing at the front. How different would the results be with another method to account for this buttressing?

Reply: Our parameterization of mélange buttressing is similar to Nick et al. (2013), which also alters the stress balance at calving front. We have not run other simulation types, but the results could be compared with other authors, as we do in the discussion section.

p.8 l.152: How much buttressing does this represent? What would be the equivalent ice thickness needed to get a similar buttressing?

Reply: For example, in 2004 our buttressing parameterization gives a longitudinal resistance that equals to 0.18 times of the driving force at calving front (Eq. 10).

p.9 l.156-157: What is this runoff symbol?

Reply: We changed this symbol to 'R'**.**

p.9 l.163 and l.175: How do you link the far ocean field temperatures to the ocean temperature in the fjord and then the temperature at the grounding line?

Reply: We add this sentence to the text:

T_f is the far field ocean forcing temperature, taken in Disko Bay (CTD in Fig. 1), relative

to pressure melting temperature under the ice shelf. Thus T and T_f are related simply by ice depth and salinity

p.10 l.178: The depth of the ocean temperatures used should depend on the geometry of the fjord, including the highest depths of the sills. What is the depth of the ocean floor in Jakobshavn's fjord, and are there sills blocking the entry of the deepest waters?
Reply: Yes. We add:
Local ocean circulation in Ilulissat fjord driven by buoyancy plume brings deep water from outside to the grounding line of Jakobshavn, and renews the fjord within 90 days in summer (Gladish et al., 2015). Generally, Jakobshavn's fjord is ~ 800 m deep but with a sill of only ~ 200 m depth at its entrance. The deepest water outside the sill can flow over the sill and reach the grounding line of Jakobshavn (Gladish et al., 2015).

p.10 l.186: "last 2 decades" while the rest of the paper rather show results since 2004.
Reply: "last 2 decades" is now "last decade".

p.10 l.187: "bedrock topography and ice thickness data in the year 2009 come from Gogineni et al. (2012)": As mentioned above, why use this dataset and not the more recent Bamber et al. (2013) or Morlighem et al. (2017) topography? Also, is this the same dataset as Jakobsson et al. (2012) shown of figure 1?
Reply: Our glacier geometry data (Gogineni et al., 2012) is derived from the same institution's products as used in BedMachine V3 with data processed by the Center for Remote Sensing of Ice Sheets (CReSIS, Leuschenetal., 2010 updated 2016). For computing resource considerations, we chose the earlier product because it has 500-meter-resolution. You may notice that Jakobsson et al. (2012) provides ocean bathymetry data (sea floor elevation).

p.10 l.192-193: I am not sure to agree with this statement: the glacier was continuing to change following its ice tongue collapse as shown in Joughin et al. (2012).
Lines are: "The aim of this initialization was provide a state rather similar to 2004, that is barely retreating on inter-annual scales (Joughin et al., 2010) and small changes of annual mean velocity in the following 3 years. Therefore"
Reply: Agreed, the statement was imprecise. The annual minimum extent of Jakobshavn retreats ~ 2 km from 2004 to 2005 following the loss of melange butressing, but then stabilizes until 2007 (Joughin et al. 2010). Annual maximum extents are stable over the 2004-2007 period. Front velocities increase slowly from 2004-2007 (~5.9% a^{-1} Joughin et al. 2010), and the model simulated velocities increase by about 3% a^{-1}. This period of relative stability also makes 2004 a good time from which to start transient simulations.

Fig.3: the stiffening factor inferred with inverse problems is often difficult to physically explain and it is here mostly equal to 1. How different would the results be if it was just assumed to be equal to 1 everywhere and the basal traction coefficient was adjusted accordingly?

Reply: The stiffening factor deviates significantly from 1 in the fast flow region (Fig 3). We are satisfied with our inversion results, which is verified in the new Fig. S1. Our inversion followed the standard built-in procedures in BISICLES (Conford et al., 2015). Here we do not want to explore techniques of solving the inverse problem, the paper is already quite long and reasonably complex, and we think it stands on its own without this.

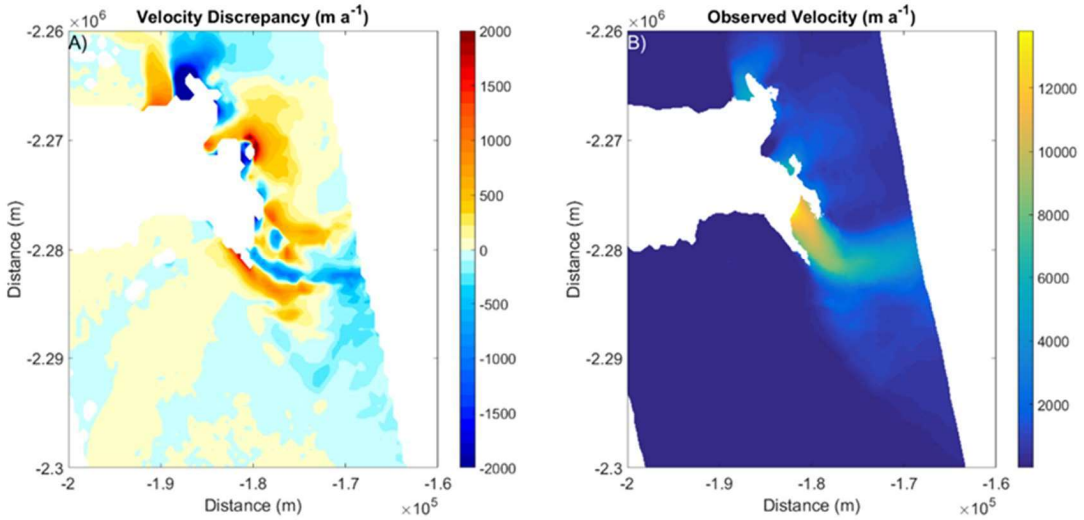

Figure S1. A) Velocity discrepancy (velocity from inversion - observed) and B) the observed velocity field (Joughin et al., 2010).

p.11 l.199-200: Why are the velocity from 2010 and the geometry from 2009 used in the inverse problem why the simulation is initialized to reproduce 2004?
Reply: There are no thickness data available for 2004. Our initializing procedure aims at rebuilding the geometry of 2004 from the closest dataset available (Gogineni et al., 2012).

p.12 l.201: "friction coefficient" and stiffening factor
Reply: Agreed. Done.

p.12 l.210: Why is the model run until the profile matched the 1998 profile? I thought the target date was 2004?
p.12 l.211: How is it changed exactly?
p.12 l.214: Are you trying to get a stable state (How do you define stable by the way? What are the variables considered?) or to match the 2004 front position? I am also a little surprised that you are mentioning a "stable state" as the glacier has been continuously since at least the 90's.
Reply: These questions are moot now as we rewrote section 2.3 (see above) in response to both yours and the other referee's confusion.

p.14 l.254: Why is considered to be the total calving? Is it the difference between the ice front positions in 2013 and 2004 or the sum of the annual ice front change position?
Reply: Line 254 now becomes:

1. Total calving front retreat from 2004-2013 measured by the difference between 2004 and 2013's annual maximum extent.

p.16 Fig.5a: There was an earlier mention of the relative stability after 2004, but this figure actually tends to show that there is not much stability at this period, with the summer front position retreating more every year.

Reply: Agreed. We have rewritten this: The annual minimum extent of Jakobshavn retreats ~ 2 km from 2004 to 2005 following the loss of melange butressing, but then stabilizes until 2007 (Joughin et al. 2010). Annual maximum extents are stable over the 2004-2007 period. Front velocities increase slowly from 2004-2007 (~5.9% a^{-1} Joughin et al. 2010), and the model simulated velocities increase by about 3% a^{-1}. This period of relative stability also makes 2004 a good time from which to start transient simulations. December front positions during 2004-2006 are close to stable, which are reproduced in our initialization procedure step 3. Notice observation extends no further prior to the summer of 2004.

p.18 Fig.6: Is it the bottom or the 300 m depth temperature?
Reply: The 300 m depth. We see the confusion with the right hand y-axis mis-labelled in Fig. 6. This has been corrected.

p.19 l.312, 314, 318: What GCM was used to force RACMO?
Reply: We change the sentence to include HadGEM2-ES here.
Figure 6. Climate forcing for future projection under the RCP4.5 scenario taken as 300 m depth ocean temperatures from HadGEM2-ES (orange) compared with the ensemble mean (red) of 7 Earth System Models (HadGEM2-ES, BNU-ESM, MIROC-ESM, IPSL-CM5A-LR, CSIRO-Mk3L-1-2, NorESM1-M and MPI-ESM-LR), (right axis), with their linear trends. Annual maximum monthly surface water run-off near Jakobshavn Isbrae's terminus from RACMO (forced by outputs from HadGEM2-ES) is shown in blue.

p.19 l.303: change reference: Joughin et al. (2010) probably did not guess what would happen in the 2013-2017 period.
Reply: Yes, but the dataset is updated to include the more recent period and is still cited as Joughin et al. (2010). https://nsidc.org/data/nsidc-0481. So we think our usage is quite standard.

p.20 l.326-329: are these results shown on a figure?
Reply: Yes. Please see new Fig. 7.

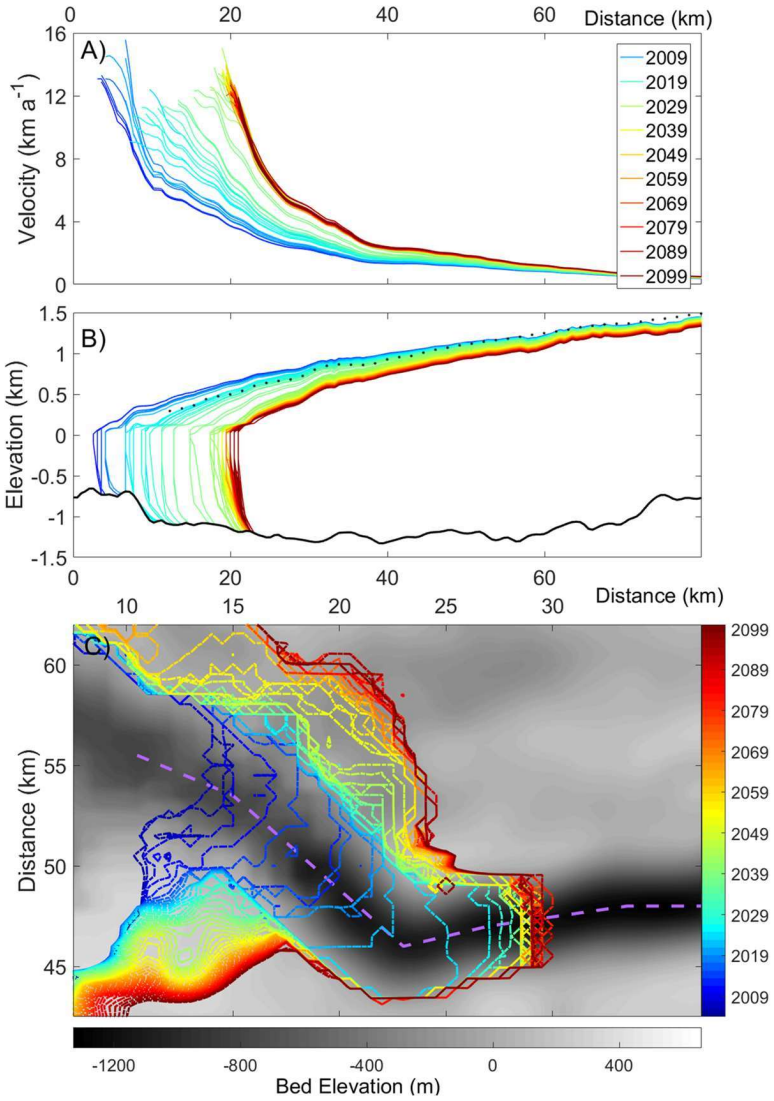

Figure 7. Modeled profiles of (A) January velocity and (B) January surface elevation along the center-flow-line (purple dash line in panel C) of Jakobshavn Isbræ from 2004 to 2099 for the RCP4.5 scenario. Bedrock elevation is shown in black. Black dotted line is the surface elevation profile extracted from radar data measured around 2010 (Gogineni et al., 2012). Profiles are shown at intervals of 1 years. Profiles are color-coded in the legend and range from blue to green and red. (C) Modeled July front positions (color bar) over its bedrock (grayscale bar) at intervals of 2 years.

p.20 Table 1 and lines 335-341: the numbers in the table and in the paragraph are somehow different (2068 vs 2029 Gt of mass loss by 2100 for example), but I might have missed something. It would also be appropriate to add the results from Bondzio et al. (2018) in the comparison here.

Reply: Sorry, 2029 should be 2068. We add a sentence in this paragraph:

Another SSA model (Bondzio et al., 2018) projects larger retreats than ours, and uses a calving parameterization that predicts the location of calving depending on tensile stress distribution, regardless of ice thickness. Their calving criterion implies a nonlinear relationship between crevasse depth and stress, compared with our linear dependence

(Eq. 12). We suggest that this nonlinearity might lead to overestimated retreats.

p.22 l.384: Does the fast flow go all the way to the sides of the fjord? It is a bit surprising to me that the bedrock provides so little resistance compared to the sides.
Reply: The basal trough beneath Jakobshavn is quite deep and narrow, which makes large velocity gradients perpendicular to flow direction at the two sides of the trough.

p.22 l.399: Is it possible to test this assumption of the impact of the shear-margin weakening mechanism?
Reply: Not possible because we cannot measure the ice viscosity directly. We made cross model comparison between ours and Bondzio et al., (2016).

p.26 l.448: There may also be some limitations associated with the initial conditions (ice too thick close to the ice front as shown on Fig.7).
Reply: Yes. We add a sentence here:
One reason for the discrepancy may be errors in initial ice thickness and real geometry in 2004.

p.26 l.462: "stimulate" → "simulate"
Reply: Done.

p.28 l.496: Did you use each GCM individually or used the mean of the 7 models?
Reply: We modify this sentence to say:
We project Jakobshavn Isbræ's future dynamic changes with climate forcing data from RACMO (2014-2099) and an ensemble mean of 7 Earth System Models for the RCP4.5 scenario.

Simulated retreat of Jakobshavn Isbræ during the 21st century

Xiaoran Guo[1], Liyun Zhao[1], Rupert ~~GladStone~~[2]Gladstone[2], Sainan Sun[3], John C. Moore[1,2,4]

[1]College of Global Change and Earth System Science, Beijing Normal University, Beijing 100875, China

[2]Arctic Centre, University of Lapland, P.O. Box 122, 96101 Rovaniemi, Finland

[3]Laboratoire de Glaciologie, Université libre de Bruxelles, Brussels, Belgium

[4]CAS Center for Excellence in Tibetan Plateau Earth Sciences, Beijing 100101, China

Correspondence to: John C. Moore (john.moore.bnu@gmail.com)

Abstract

~~The e~~Early in the 21st century retreat of Jakobshavn Isbræ, one of Greenland's largest outlet glaciers, into its over-deepened bedrock trough was accompanied by acceleration to unprecedented ice-stream speeds. Such dramatic changes suggested the possibility of substantial mass loss over the rest of this century. Using a three-dimensional ice-sheet model with parameterizations to represent the effects of ice mélange buttressing, crevasse-depth-based calving and submarine melting, we can reproduce its recent evolution. The model can accurately replicate its inter-annual variations in grounding line and terminus position, including new modes of seasonal fluctuations that emerged after arriving at the over-deepened basin and the disappearance of a persistent floating ice shelf. The shear margin induced decreases in ice viscosity we simulate are particularly important in reproducing the large observed inter-annual changes in terminus velocity. We use this model to project Jakobshavn's evolution over this century when forced by the IPCC RCP4.5 climate scenario and simulated by ocean temperatures from 7 Earth System Models along with surface runoff derived

from RACMO. In our simulations, Jakobshavn's grounding line continues to retreat ~ 18.5 km by the end of this century ~~with~~leading to a total mass loss of ~ ~~2030~~2070 Gt (5.~~6~~7 mm sea-level-rise equivalent). Despite the relative success of the model in simulating the recent behavior of the glacier, the model does not simulate winter calving events that have become relatively more important.

1 Introduction

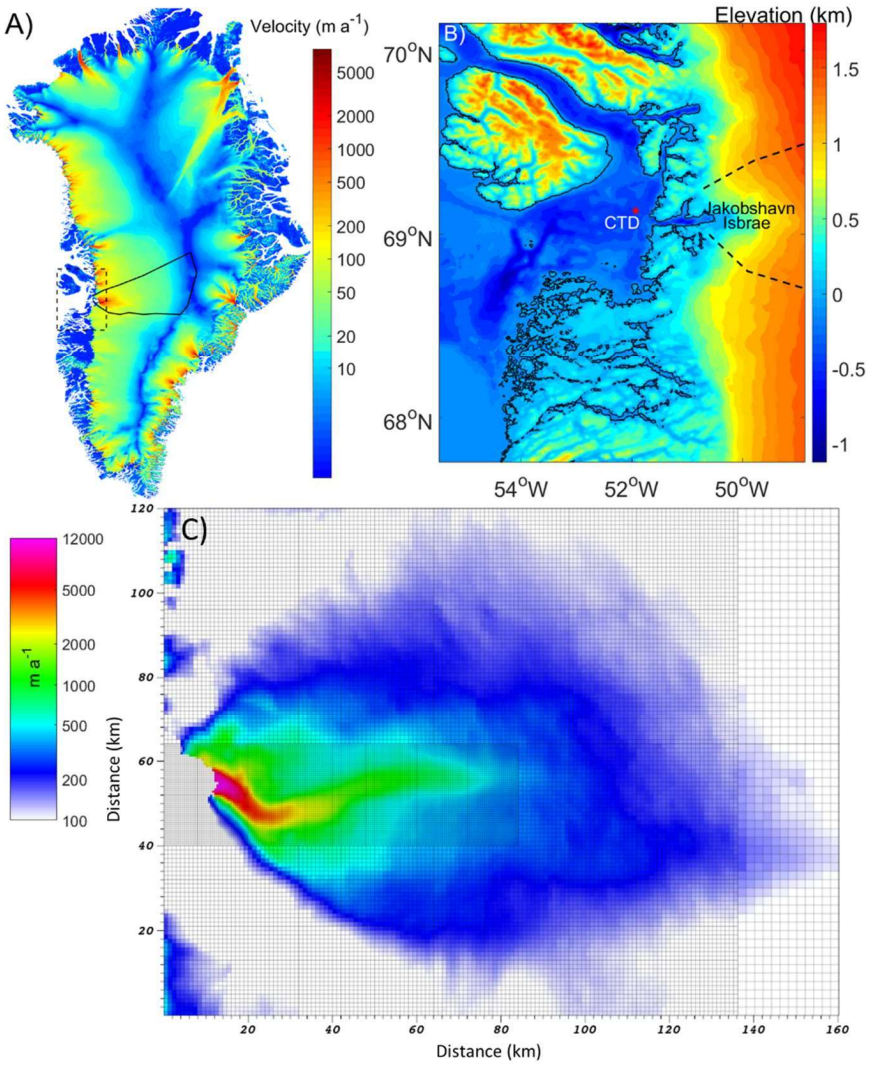

Figure 1. A) Greenland ice sheet flow speeds from Joughin et al. (2018), with the Jakobshavn drainage basin outlined by the solid black line and the area shown in panel B by the dashed box. B) Ilulissat Fjord and Disko Bay bathymetry from Jakobsson et al.

(2012), with the CTD (Conductivity Temperature Depth) site used for ocean temperature here marked by the red star. C) Example of the mesh used with finest resolution of 500 m with modeled velocities at the beginning of 2004.

Jakobshavn Isbræ (Fig. 1) is Greenland's largest and fastest outlet glacier, with transient speeds of up to 17 km a^{-1} (Joughin et al., 2014). Jakobshavn Isbræ drains ~ 6.5 % of the Greenland Ice sheet (Krabill et al., 2000), and it alone contributed ~ 1 mm to global sea-level rise between 2000 and 2011 (Howat et al., 2011). Since 1997, measurements indicate that the water entering Ilulissat Fjord where Jakobshavn Isbræ terminates, is about 1.1 ºC warmer than it was during 1987-1991 (Holland et al., 2008). This rise in water temperature coincided with the onset of dramatic thinning, speedup and retreat of Jakobshavn Isbræ. By 2003 its velocity near the grounding line had reached ~ 12.6 km a^{-1}, more than double that of 1992, and the floating ice mélange in the fjord had disintegrated (Joughin et al., 2004). From 2005 to 2007, as it retreated inland, seasonal fluctuations in velocity 4 km inland from the calving front amounted to ± 1 km a^{-1}. The winter slowdowns and summer accelerations occurred in tandem with the calving front winter advance and summer retreat. By 2012 the seasonal velocity fluctuations 4 km upstream from the calving front ~~was~~ were nearly ± 8 km a^{-1} and the grounding line of Jakobshavn Isbræ had reached the bottom of a sub-glacial bedrock trough after years of down-slope migration (Joughin et al., 2014).

Before 1997, Jakobshavn ~~possessed~~had a ~ 15 km long floating ice mélange in front of its terminus ice cliff and experienced submarine melting on its ice-ocean interface (Amundson et al., 2010). After 1998 the terminus became more crevassed, coinciding with acceleration of the glacier, implying that weakened buttressing had triggered its dramatic speed-up. A thinning rate of 230 ± 50 m a^{-1} between the summers of 1984 and 1985 was deduced from photogrammetric surveys, mostly due to submarine melting (Motyka et al., 2011). The floating tongue thickened during the mid-1990s followed by progressive thinning after 1997 (Motyka et al., 2011). From 1997 to 2008, the average ocean temperature was 1.1°C higher than during the period 1980 – 1991, which raised its thinning

rate substantially, affecting the whole ice mélange, and the ice shelf eventually collapsed in 2003. Many lines of evidence suggest that warm water was responsible for the submarine melting beneath the ice mélange and ice-shelf, brought by a buoyancy-driven, overturning circulation in Ilulissat fjord (Gladish et al., 2015).

Jakobshavn, in common with most outlet glaciers in Greenland, flows through a narrow, deeply incised bedrock trough at a ~~far~~much faster rate than the ice surrounding it (Joughin et al., 2010). Gravity surveys suggest a deep layer of soft till underlies much of the Jakobshavn trough (Block and Bell, 2011). This soft bed provides almost no resistance to ice flow and basal shear stress maps show that most of the gravitational driving force on the glacier is balanced by lateral drag (Shapero et al., 2016).

Basal drag decreased from 1995 to 2006 (Habermann et al., 2013), possibly due to fast thinning that reduced the effective pressure, that is the ice overburden minus water pressure, at the bed. The effective pressure distribution under the glacier is important to basal drag and ~~must be~~~~it is~~approaches zero at the grounding line as it begins to float. Several sliding parameterizations (also termed sliding relations or sliding laws) have been used in the literature that assume basal drag depends on sliding speed (so-called Weertman sliding (Weertman, 1957)), or on effective pressure (Schoof, 2010; Gagliardini et al., 2014). Tsai et al. (2015) introduced a combined Weertman and Coulomb sliding law based on effective pressures with a boundary layer at the grounding line; this has a higher scaling of ice flux with grounding-line thickness compared with the Weertman. However, in the Jakobshavn case, both Weertman and Coulomb sliding produce very similar fluxes because the basal shear stresses along the main trough are typically only 2-% of the driving force~~.~~ (Shapero et al., 2016).

Simulations using a flow-band model with a crevasse-depth-based calving parameterization (Vieli et al., 2011) demonstrated that loss of buttressing from the ~~disintegration of its floating~~

~~ice~~weakening mélange or enhanced submarine melting could have triggered the dramatic changes seen in Jakobshavn Isbræ at the end of the 20th century. Later work (Muresan et al., 2016), using a simple calving model with dependence on the strain field at the terminus was able to reproduce the inter-annual retreat of Jakobshavn Isbræ until 2009, when the terminus arrived at the beginning of the reverse sloping bed. But retreat after 2010 was not captured by their model, and neither ~~was~~ were the seasonal fluctuations in terminus position. Bondzio et al. (2018) applied a similar calving model that removes any ice where tensile stress exceeds a threshold, as simulated with a SSA (Shallow Shelf Approximation) model, regardless of ice thickness. To represent seasonal fluctuation of front position, their stress threshold is a stepwise constant function in time with low values in summer. After calibration, their model can closely reproduce the observed behavior from 1985 to 2018 when forced only with ocean temperatures.

In this paper we use a three-dimensional ice-flow model with a treatment of calving that successfully tracks the seasonal terminus position and its retreat into the over-deepened basin. We use historic observations of ocean temperature as forcing and ice tongue thinning rate to scale submarine melting rates for our model and thence make future projections. Our aim is to track the evolution of Jakobshavn Isbræ through the 21st century under a specific climate forcing scenario. In Section 2 we describe the approach and calibration of our model, Section 3 shows the simulations for the period to 2100 under the IPCC RCP4.5 scenario (Moss et al., 2010), Section 4 is a discussion of our method with reference to other studies and suggestions for improvements, and we conclude in Section 5.

2 Methods and data

2.1 Ice sheet model

We model Jakobshavn Isbræ using the BISICLES ~~continuum~~ ice sheet dynamics model that is based on the vertically integrated stress balance formulation of Schoof and Hindmarsh (2010), which treats longitudinal and lateral stresses as depth-independent, but allows for vertical shear in the nonlinear rheology (Cornford et al., 2013). BISICLES is particularly useful for Jakobshavn Isbræ as it uses block-structured finite volume discretization with adaptive mesh refinement (Cornford et al., 2013) allowing for high resolution modeling of critical sections of the glacier. Jakobshavn Isbræ is fed by a ~ 400 km long and extensive drainage basin (Fig. 1), but the fast flow area is only around 10 km in width. Our highest mesh resolution of 500 m is used to cover the whole fast-flow-area including the shear margin (Fig. ~~S~~1c), while the rest of the glacier is modeled at 1000 m resolution.

We assume Jakobshavn Isbræ to be in hydrostatic equilibrium, thus the upper surface elevation s is

$$ss = \max\left[h + b, \left(1 - \frac{\rho_i}{\rho_w}\right) h\right] \max\left[h + b, \left(1 - \frac{\rho_i}{\rho_w}\right) h\right], \quad (1)$$

where ρ_i ρ_i and ρ_w ρ_w are the densities of ice (917 kg m^{-1}) and ocean water (1027 kg m^{-1}), h is ice thickness and b is bedrock elevation relative to sea level. The ice thickness evolves in time as

$$\frac{\partial h}{\partial t} + \nabla \cdot [\mathbf{u}h] = M_s - M_b, \frac{\partial h}{\partial t} + \nabla \cdot [\boldsymbol{u}h] = M_s - M_b, \quad (2)$$

where M_s, M_b are surface mass balance (SMB) and submarine melt rate respectively and $\boldsymbol{u}$ is the depth-independent horizontal velocity. No basal melting over the grounded area is allowed. The velocity $\boldsymbol{u}$ satisfies an approximate stress balance equation (Schoof and Hindmarsh, 2010)

$$\nabla \cdot [\phi h\bar{\mu}(2\dot{\epsilon} + 2\mathrm{tr}(\dot{\epsilon})\mathrm{I})] - \tau^b = \rho_i g h \nabla s, \quad (3)$$

where $\mathbf{I}$ is the identity tensor, s is the ice surface elevation, g is the acceleration due to gravity, $\dot{\boldsymbol{\epsilon}}$ is the horizontal strain-rate tensor defined by

$$\dot{\epsilon}\dot{\epsilon} = \frac{1}{2}[\nabla \mathbf{u} + (\nabla \mathbf{u})^{\mathrm{T}}][\nabla \boldsymbol{u} + (\nabla \boldsymbol{u})^{\mathrm{T}}], \quad (4)$$

and τ^b is the basal shear stress. The vertically integrated effective viscosity $\phi h\bar{\mu}$ is given by

$$\phi h\bar{\mu}(x,y) = \phi \int_{s-h}^{s} \mu(x,y,z)\mathrm{dz}, \quad (5)$$

where the vertically varying effective viscosity μ includes a contribution from vertical shear and satisfies

$$2\mu A(T)(4\mu^2\dot{\epsilon}^2 + |\rho_i g(s-z)\nabla s|^2)^{(n-1)/2} = 1, \quad (6)$$

where n is the flow rate exponent, set to 3 in the current study, and $A(T)$ is the rate factor, dependent on the ice temperature T through an Arrhenius law (Cuffey and Paterson, 2010). ϕ is a stiffening factor estimated by solving an inverse problem (Cornford et al., 2015) using measured surface velocities.

We use a viscous Weertman sliding relation to define the basal friction:

$$\tau^b = \begin{cases} -C|\boldsymbol{u}|^{m-1}\boldsymbol{u} & \text{if } \frac{\rho_i}{\rho_w} h > -b \\ 0 & \text{otherwise} \end{cases}, \quad (7)$$

and here we assume a linear relation taking m=1. The basal traction coefficient C(x, y) is estimated simultaneously with the stiffening factor ϕ by solving the inverse problem (Cornford et al., 2015). C and ϕ are adjusted iteratively to reduce the misfit with a set of 2010 surface velocity observations (Joughin et al. 2010). We hold the fields C and ϕ constant over time

throughout our simulations, although they must actually change as the glacier retreats. We also do not thermomechanically couple the model, but use a constant ice temperature of -10°C.

Reflection boundary conditions were applied at the edge of ~~each~~ the domain:

$$\boldsymbol{u}\cdot\boldsymbol{n}=0,\qquad \boldsymbol{t}\cdot\nabla\boldsymbol{u}\cdot\boldsymbol{n}=0,\qquad \nabla h\cdot\boldsymbol{n}=0, \quad (8)$$

where $\boldsymbol{n}$ is normal to a boundary and $\boldsymbol{t}$ is parallel to it. Normal stress across the calving front is equal to the hydrostatic water pressure there:

$$\boldsymbol{n}\cdot[\phi h\bar{\mu}(2\dot{\boldsymbol{\epsilon}}+2\mathrm{tr}(\dot{\boldsymbol{\epsilon}})\mathbf{I})]-\boldsymbol{\tau}^{b}=\frac{1}{2}\rho_i \mathrm{g}\left(1-\frac{\rho_i}{\rho_w}\right)h^2\boldsymbol{n}. \quad (9)$$

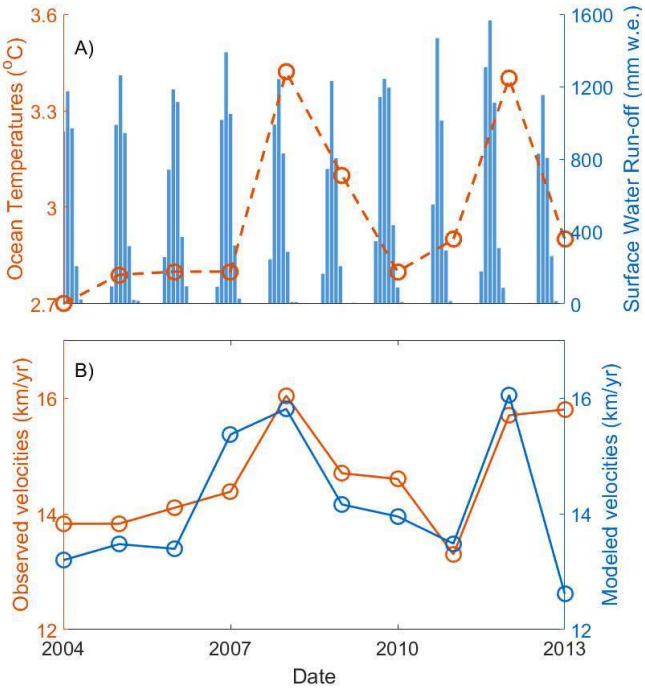

Figure 2. A) Time series of observed ~300 m deep ocean temperature (red) from ~~http://ocean.ices.dk/HydChem/~~ near the mouth of Ilulissat fjord (See Fig. 1 for location). Blue bars are simulated monthly surface water run-off from the MAR regional surface mass and energy balance model (Alexander et al. 2016). B) Measured ice front annual mean ice flow speeds (red) from Joughin et al. (2010), compared with our modeled speeds (blue).

2.2 ~~Climate~~ Forcing

Local ocean circulation in Ilulissat fjord driven by buoyancy plume brings deep water from outside to the grounding line of Jakobshavn, and renews the fjord within 90 days in summer (Gladish et al., 2015). Generally, Jakobshavn's fjord is ~ 800 m deep but with a sill of only ~ 200 m depth at its entrance. The deepest water outside the sill can flow over the sill and reach the grounding line of Jakobshavn (Gladish et al., 2015). We use 300 m depth ocean temperatures collected from a CTD site close to the mouth of Ilulissat fjord (Fig. 1) as an approximation of ocean temperatures near the glacier grounding line~~. A comprehensive study focusing on ocean circulation within Ilulissat fjord validated this approximation~~ (Gladish et al. 2015). A positive correlation ($r=0.74$, $p<0.05$) exists between deep ocean temperatures and flow speed near the terminus of Jakobshavn Isbrae (Fig. 2) from 2004 onwards. There is no significant correlation prior to 2004, the floating ice tongue period. As a working hypothesis we assume that the correlation since 2004 reflects the effects of the sea ice and iceberg mélange in the fjord on the flow speed near the terminus: a warmer ocean reduces mélange thickness and therefore buttressing. There appears to be no lag between the glacier acceleration and change in deep ocean temperature, suggesting mélange response times are faster than 1 year. When the floating ice tongue was present lags in the system were likely longer, accounting for the lack of correlation between ocean temperatures and glacier flow speed prior to 2004. It is also possible that ocean temperatures reflect changes in surface runoff and basal lubrication for sliding, but we consider that the runoff more strongly affects calving mechanisms as discussed later. We therefore modify the driving force (Eq. 3) on the grid cells next to the calving front by multiplying by a factor α ~~(tuned value shown by Eq. 9~~ that is linearly related to ocean temperature (T) as a means of representing the buttressing effects of the ice mélange in the fjord.

~~$$\nabla \cdot \left[\phi h \overline{\mu} (2\dot{\epsilon} + 2\mathrm{tr}(\dot{\epsilon})\mathrm{I})\right] + \tau^b = \alpha \cdot \rho_i g h \nabla s, \quad (8)$$~~

~~$\alpha = 0.82 + 0.111 \cdot T$, (9)~~

~~We use a crevasse based calving parameterization (Benn et al., 2007; Nick et al., 2011~~ $\nabla \cdot [\phi h \bar{\mu}(2\dot{\epsilon} + 2\mathrm{tr}(\dot{\epsilon})\mathbf{I})] + \boldsymbol{\tau}^b = \alpha \cdot \rho_i g h \nabla s$, (10)

$\alpha = \alpha_1 + \alpha_2 \cdot T$, (11)

The coefficients α_1 and α_2 are tunable with limits based on observations as discussed later in Section 2.4. –This approach is similar to Nick et al. (2013), which also alters the stress balance at calving front. Our buttressing parameterization gives a longitudinal resistance that is 18% of the driving force at calving front (Eq. 10), for the instance of 2004.

We use a crevasse based calving parameterization (Benn et al., 2007; Nick et al., 2013) that calves ice where the crevasse penetration depth (D_s) is greater than upper surface elevation. D_s is defined as

~~$D_s = \frac{S}{g \cdot \rho_i} + \frac{\rho_w}{\rho_i} \cdot R \cdot \beta$, (10)~~

$D_S = \frac{S}{g \cdot \rho_i} + \frac{\rho_w}{\rho_i} \cdot \mathrm{R} \cdot \beta$, (12)

where S is the magnitude of extensional stress, ~~R~~ R is surface water run-off, and β is a tuning scalar. We estimate runoff from the 25 km resolution regional climate model, MAR, (Alexander et al. 2016), driven by the ERA-Interim reanalysis (Dee et al., 2011).

We characterize submarine melting as a linear function of ocean forcing

$M_b = \gamma T_f$, (~~11~~13)

where T_f is the far field ocean forcing temperature, taken in Disko Bay (CTD in Fig. 1), relative to

pressure melting temperature under the ice shelf. Thus T and T_f are related simply by ice depth and salinity. We derive γ (Section 2.3) from the 1985 observed submarine melt rate of 1 ± 0.2 m day^{-1} beneath the floating ice mélange of Jakobshavn Isbræ, when Disko Bay ocean temperatures were 4.2°C warmer than the pressure melting point at the bottom of the floating ice shelf (Motyka et al. 2011). We test the sensitivity of the modeled glacier to uncertainty in submarine melt rate in section 2.4.

We force Jakobshavn Isbræ in the 21st century using SMB and run-off from the 11 km resolution RACMO model (Van Angelen et al., 2013) driven by the RCP4.5 scenario (Moss et al. 2010). The run-off values are averaged over the nine grid points nearest to the terminus of Jakobshavn (69.1°N, 50.0°W). In general we use RACMO products to drive the model, however they only span the period of 2006-2099. For the period 2004-2014, SMB and surface water run-off forcing come from MAR model outputs~~. Because RACMO outputs cover only the period of 2006-2099. For the period 2015-2099, our SMB and run-off forcing are from RACMO outputs.~~. We use the common overlapping period (2006-2014) to correct the bias between two models outputs. The RACMO simulation was forced by the HadGEM2-ES Earth system model (Collins et al., 2011), as this climate model was found to be the most realistic for present-day simulations of the Greenland ice sheet (Van Angelen et al., 2013). Ocean forcing in Equations 10 and 13 should relate to temperatures off the continental shelf close to the fjord mouth. Cowton et al. (2018) achieved success in simulating the terminus position and yearly variability of 10 glaciers along the east coast of Greenland using mean 200-400 m depth temperatures from reanalysis data. For consistency with the RACMO results, we use deep ocean temperatures at ~ 300 m depth from the 0.83°×1° resolution HadGEM2-ES driven by the RCP 4.5 climate scenario from 2005 to 2100 at the 3 closest grids point to Disko Bay. We also compare this with results from 7 other climate model simulations of RCP4.5: HadGEM2-ES (Collin et al., 2011), BNU-ESM (Ji et al., 2014), MIROC-ESM (Watanabe et al., 2011), IPSL-CM5A-LR

(Dufresne et al., 2013), CSIRO-Mk3L-1-2 (Gordon et al., 2002), NorESM1-M (Bentsen et al., 2012) and MPI-ESM-LR (Giorgetta et al., 2013).

2.3 Initialization Procedure

As we are interested in high resolution simulations and validating our model parameterizations with observations over the last ~~2 decades~~decade, we take care to initialize the model as accurately as possible. Detailed bedrock topography and ice thickness data in the year 2009 comes from Gogineni et al. (~~2013~~2012); we chose the product because it has 500 m resolution and so matches the highest resolution of~~.~~ our mesh. Jakobsson et al. (2012) provides ocean bathymetry data (Fig. 1). In 2004 the floating ice shelf disintegrated, making it a convenient starting point for simulations since we might expect the system to respond differently to forcing when there was a floating ice shelf compared with the situation of ocean forcing along a near-vertical ice cliff. This is consistent with the observed good correlation between ocean temperature and flow speed after 2004 but not before. The aim of this initialization was provide a state rather similar to 2004, that is barely retreating on inter-annual scales (Joughin et al., 2010) and small changes of annual mean velocity in the following 3 years. Therefore

1) We solved the inverse problem for basal conditions (Eq. 7) and stiffening factor using 2010 velocities (Joughin et al., 2010) and 2009 geometry (Gogineni et al., ~~2013).~~ 2012), following Cornford et al. (2015). Our friction coefficient ~~field is~~and stiffening factor fields are shown in Fig. 3. Fig. S1~~2~~ shows the discrepancy between observed velocity field (Joughin et al., 2010) and the velocity derived from the inversion.

~~2) We made an initial guess for β (Eq. 10) based on short (less than one decade) transient simulations incorporating calving but not SMB or ice shelf melt forcing, starting from our~~

~~inverted model state from step 1 above. This was forced by seasonal repetitions of runoff from MAR for the year 2010.~~

~~3)~~2) Starting from the inversion of step 1 ~~and using β (Eq. 10) from step 2~~, we let the model glacier evolve freely without calving and with zero SMB and with sub-shelf melting (γ=0.0238) forced by repeating the observed 2004 ocean temperature for 11 years ~~(that means the coefficient γ in Eq. 11 was set to be 1)~~ until its surface elevation profile ~~was similar to the known profile of 1998 (Bamber et al. 2001).~~ reached a state shown in Fig. S2~~3~~.

~~4)~~3) We carried out several 10-year simulations each with different β ~~gradually decreased from its initial value given by step 2, to 45% of this value.~~values ~~estimated.~~ These simulations were forced by repeatedly applying the 2004 seasonal climate forcing~~.~~ so that the glacier approaches a steady state. From these, we selected the β that ~~best allowed Jakobshavn Isbræ to reach a stable state by the 8th year (changes in the 9th and 10th years of simulations were negligible) such that its~~provided a calving front position closest to that observed in 2004. The best β here is ~~53% of its value from step 2~~0.034, and~~.~~ ~~T~~this is our best guess for the 2004 state. The annual minimum extent of Jakobshavn retreats ~ 2 km from 2004 to 2005 following the loss of melange butressing, but ~~there~~then stabilizes until 2007 (Joughin et al. 2010). Annual maximum extents are ~~no thickness data available for 2004. Notice that~~stable over the ~~front positions and May front~~2004-2007 period. Front velocities ~~from 2004-2006 are stable (Figs 2 and~~increase slowly from 2004-2007 (~5.9% a^{-1} Joughin et al. 2010), and the model simulated velocities increase by about 3~~), suggesting that the glacier was reasonably close to steady state. This~~% a^{-1}. This period of relative stability also makes 2004 a good time from which to start transient simulations.~~–~~

Basal friction coefficient values downstream of the 2010 grounding line were set equal to that in the

nearest 2010 grounded location. This was necessary because steps 2, ~~3~~ and 43 involved grounding line advance beyond the region for which basal friction coefficients had been inferred. The geometry after this spin up procedure, and the friction coefficient and stiffening factor distribution from the inversion in step 1 were used as the initial condition for model calibration.

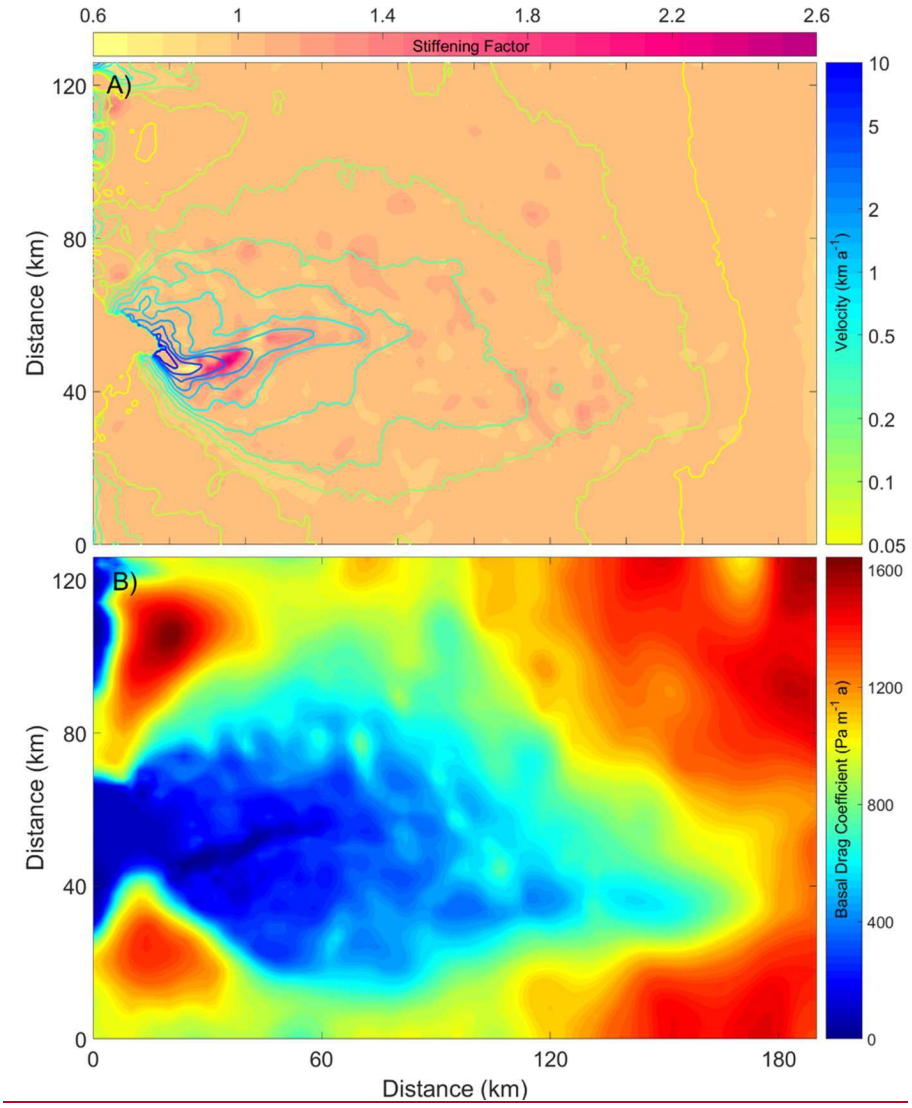

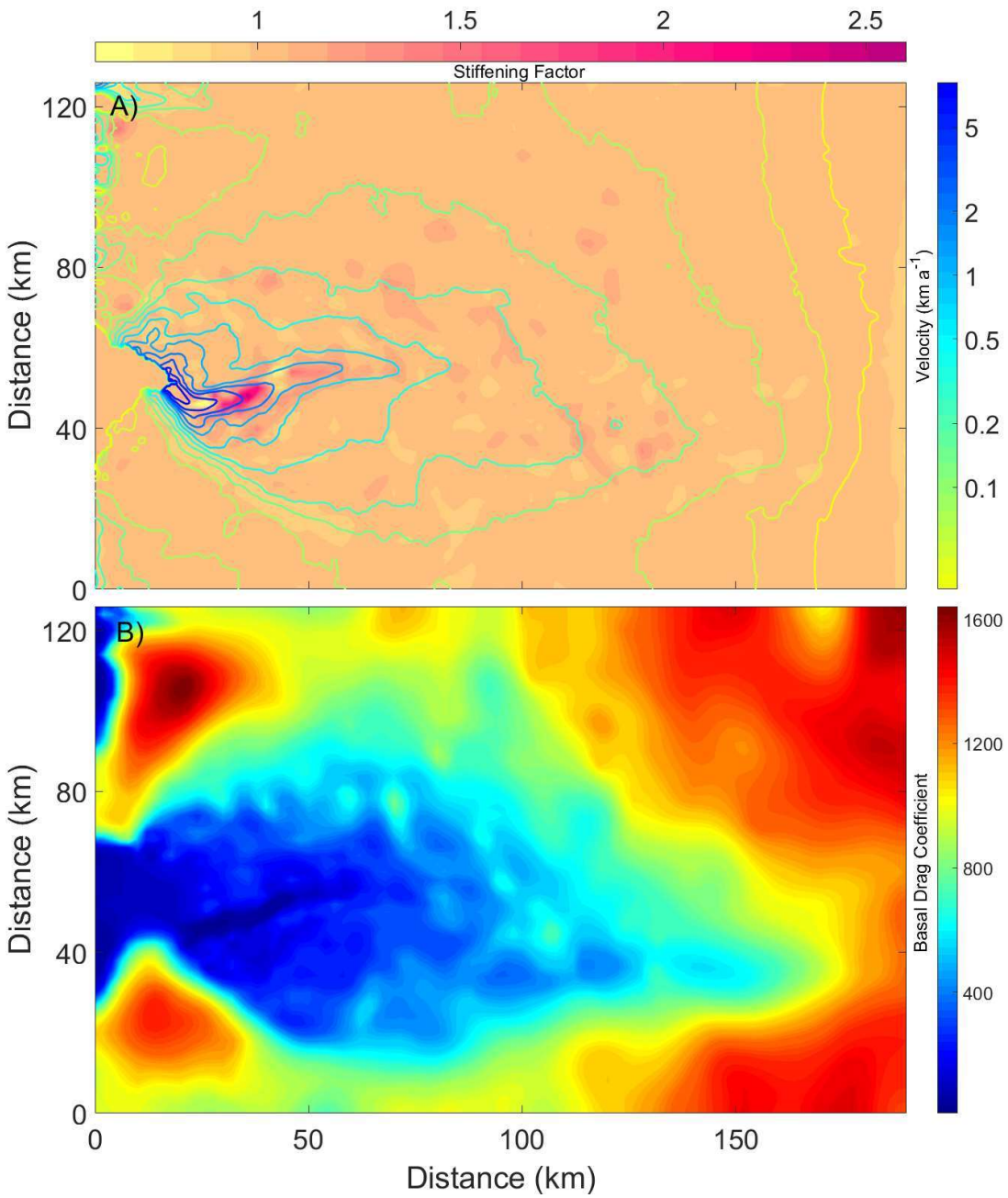

263

264 **Figure 3. (A) Stiffening factor Φ (Eq. 3) and (B) basal traction coefficient C (Eq. 7) over the**
265 **computational domain from solving the inverse problem. Contour lines in panel A show the**
266 **modeled velocity (logarithmic scale).**

267 # 2.4 Model calibration

268 ~~There are three essential~~The parameters in the model, α, β and γ representing mélange buttressing,

crevasse depth sensitivity to surface runoff, and shelf melt sensitivity to ocean temperatures~~. In the initialization, we fix γ~~ need to be ~~1. Therefore, we performed a suite~~estimated. The measured relationship between ocean temperatures and sub-shelf melt rate (Motyka et al., 2011) gives the value of ~~about 50 simulations~~γ to be 0.238. We manually tune ~~the~~ parameters in Eq. 11 and Eq. 12: ~~α~~α over the range 0.7−1.2 for α_1 and 0.09-0.12 for α_2; and ~~β with fixed γ=1. Our target was~~β (0.04 - 0.075) ~~manually~~ to best reproduce Jakobshavn Isbræ's calving front position and surface velocity evolution for the 10 year period 2004-2013. Reproducing the total retreat distance ~~of retreat~~ and the temporary stable state after 2012 were secondary desirable features to match. The best set of parameters are α_1=0.82, α_2=0.111, β=0.0638. Since these values come from a manual search we do not claim them to be the best in all parameter space. We assess model sensitivity to the parameter values next.

~~Because only within a small range of β will modeled retreats make sense, firstly we estimate reasonable range of β when hold α=1.0, γ=1.0. Secondly, we explore the parameter space centered by (α=1.0, β=0.06), which come from estimations above, to match observed retreats and general velocities neglecting the inter-annual variations. The parameter space tested here is (1.0±0.25, 0.06±0.01). As the discussion above, we further assume $\alpha = \alpha_1 + \alpha_2 T$, i.e., linearly related to deep ocean temperature. With velocity depending on ocean temperature, degree of freedom of our parameter space grow to three, which are α_1, α_2, β. However, we find β and α_2 behave quite independently within the small β range estimated so far, which allow us finally reach a set of parameters that can accurately reproduce both the total retreats and the velocity variations including inter-annual fluctuation. The tuning was implemented manually. The best set of parameters are α_1=0.82, α_2=0.111 and β=0.0638, as shown in Eq. 9.~~

We explore the glacier's sensitivity to two types of boundary perturbations. They are ice mélange

buttressing effect (defined by α) and submarine melting (defined by γ). We scaled submarine melt rates by multiplying γ by values from 0.8-1.2, based on the range of the observation uncertainty in melt of ~ 20% (Motyka et al. 2011). Also we varied α by multiplying by factors from 0.91 to 1.25 to represent different buttressing strengths (Eq. ~~8~~10). These multiplication factors were varied systematically with typical intervals of 0.1 and 0.03 respectively for the γ and α factors. We calculated the following relative mismatches defined as (model-observations)/observations for each simulation (shown in Fig 4):

1. Total calving front retreat from 2004-2013 measured by the difference between 2004 and 2013's annual maximum extent.
2. Annual mean front velocities
3. Vector sum of 1) and 2)

We used ~~β~~ β (Eq. ~~10~~12) from our optimal set of parameters. Our optimal value for α is such that a 20% rise of its value does not affect modeled retreat when ~~β~~ β and γ are kept to be their optimal values (Fig. 4 A).

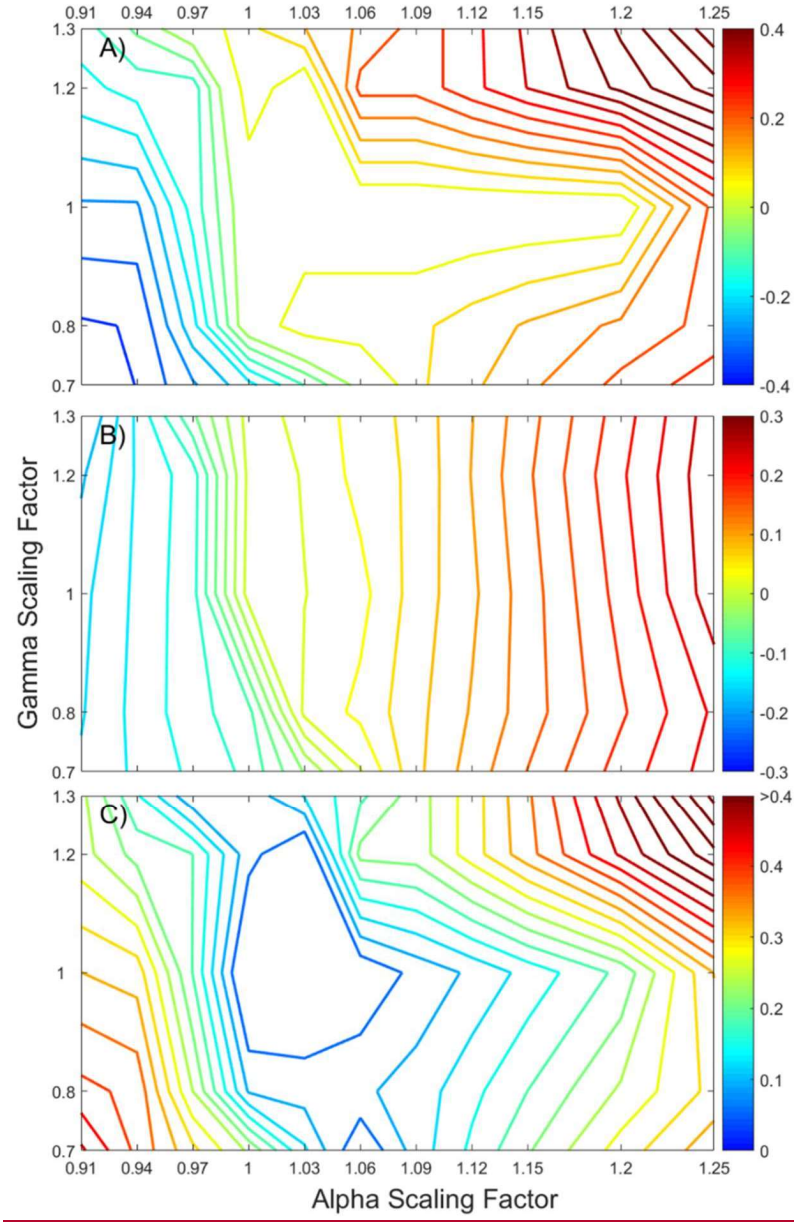

306

307 **Figure 4. Relative mismatches defined as (model-observed)/observed for A) total calving front**
308 **retreat, B) average of annual mean front velocity during 2004-2013, C) the vector sum of**
309 **mismatches in panels A and B, $\sqrt{(A^2+B^2)}$ in our 2-D parameter space ~~(α, γ) centered by the best~~**
310 **~~set ($\alpha * 1.0, \gamma * 1.0$)~~. X- and y-axis are multipliers of α and ~~γ used respectively in different~~**
311 **~~runs~~.**

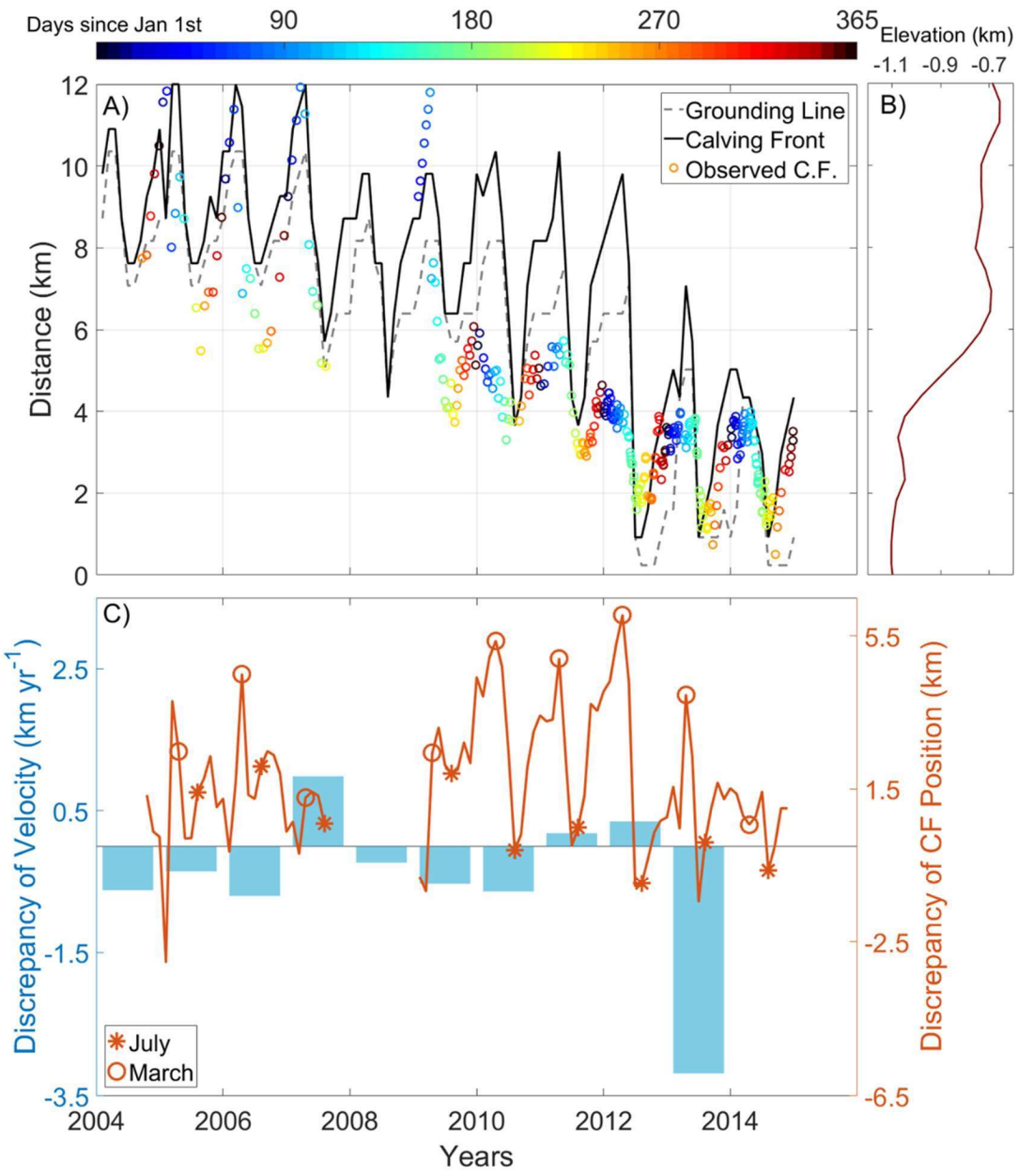

Figure 5. (A) Modeled retreat of the calving front (black solid line), grounding line (gray dashed line), and observed calving front positions (color-coded circles and scale bar) from Joughin et al. (2014). (B) Bedrock elevations. (C) Residuals (modeled minus observed) of annual mean front velocity (blue bars, left axis) and of calving front position (red lines, right axis) with typical timings of annual maximum (March) and minimum (July) extent marked. The modeled front velocities and calving positions explain about 49% and 76% of the variance in corresponding observations.

The two biggest mismatches occur with the 2007 and especially 2013 velocities (Fig. 5). 2013 has the lowest simulated surface water run-off (Fig. 2) of all the years since 2004. The Benn calving

model we use is sensitive to runoff, with reduced run-off leading to lower crevasse-penetration-depth and reduced terminus fracturing thus increasing its buttressing force. ~~In~~Furthermore 2013 had relatively cool ocean temperatures which were lower than the ~~2012/13 winter, the modeled glacier had an unprecedentedly high calving front and had been flowing fast the previous summer. This led to growth~~average of ~~an unusually long seasonal ice-shelf in the winter which caused~~ 2004-2013. The cool ocean temperatures also increased buttressing, leading to low ~~velocities near the end of front advancing season, and so accordingly low~~simulated annual mean ~~velocity. The low modeled velocity in 2009 can also be interpreted by the same over-growth effect, even though the ocean temperatures were high in 2009.~~velocities. Jakobshavn Isbræ did not in fact slow down very much in ~~2009 and~~ 2013 because there were calving events (Cassotto et al. 2015) that are unrepresented in our model. The relevant mechanisms are discussed later.

In 2007 high run-off caused more simulated calving and retreat than in reality. These retreat phases reduced the buttressing and lateral drag due to shear-margin-weakening, all of which lead to excessive speed-up near the terminus.

Modeled calving front retreat is ~ 7 km in total from 2004-2014 (Fig. 5), which is consistent with observations (Joughin et al. 2014). In 2009 a dramatic retreat brought the grounding line to the bottom of the bedrock slope, and since then it has gradually retreated with smaller seasonal fluctuations. The run-off forcing we applied triggered major retreats in the summers of 2007 and 2012, due to large summer peak run-off (Fig. 2), demonstrating the sensitivity of our calving parameterization to run-off forcing. Modeled timings of maximum extent and minimum extent each year are in good agreement with observations, also demonstrating that summer, in particular, May to July, run-off determines much of the behavior of Jakobshavn Isbræ.

The modeled range of seasonal fluctuation in front position is ~ 5 km, which is similar to

observations in the period before 2008. From January 2009 to December 2011, there was an abrupt decrease in seasonal front fluctuation, with many winter calving events occurring, in contrast with previous years (Cassotto et al. 2015). These winter calving events may explain the small observed seasonal fluctuations because they limit the winter advance. Our model is unable to stimulate these winter calving events because there is no winter run-off, and as extension stresses are never enough to cause winter calving, ~~hence~~ calving is then zero ~~then~~. The largest discrepancy of front position occurs during these winter calving periods (Fig. 5). Observations also showed that from 2013 to 2017, Jakobshavn Isbræ barely retreated (Joughin et al. 2010). The decline of run-off (Fig. 2) in 2014 suggests the reason. But since no RACMO run-off simulations are yet available for 2015 and later, our parameterizations cannot be tested against this lack of retreat.

3 Future evolution

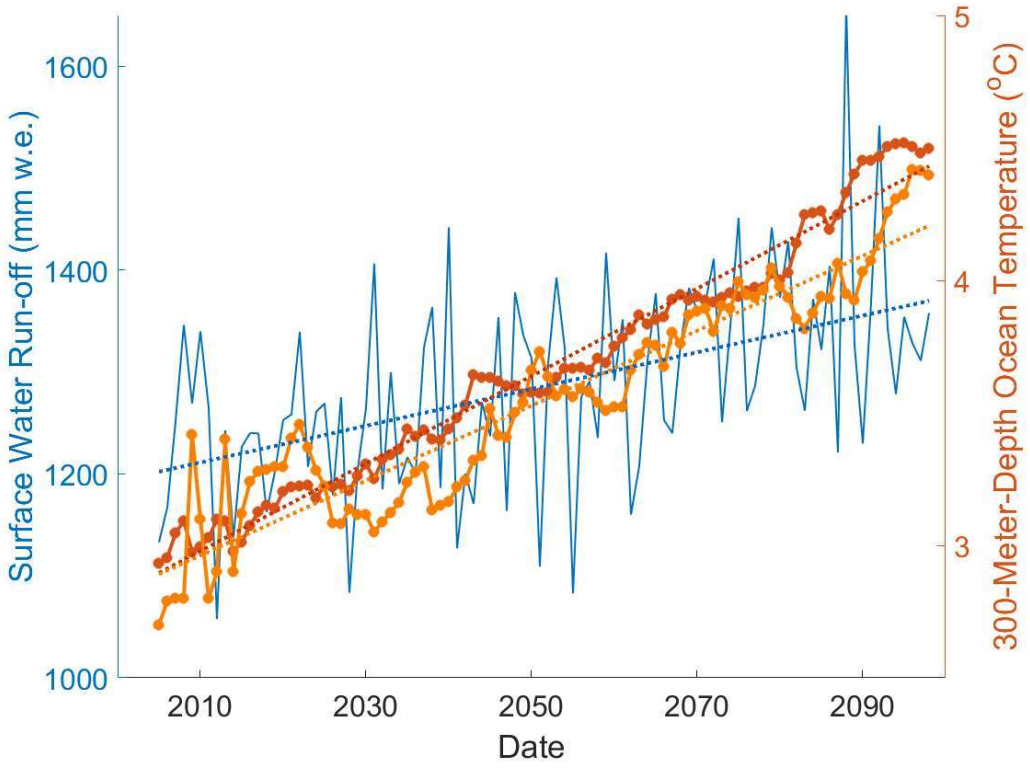

Figure 6. Climate forcing for future projection under the RCP4.5 scenario taken as 300 m depth ocean temperatures from HadGEM2-ES (orange) compared with the ensemble mean (red) of 7 Earth System Models (HadGEM2-ES, BNU-ESM, MIROC-ESM, IPSL-CM5A-LR, CSIRO-Mk3L-1-2, NorESM1-M and MPI-ESM-LR), (right axis), with their linear trends. Annual maximum monthly surface water run-off near Jakobshavn Isbrae's terminus from RACMO (forced by outputs from HadGEM2-ES) is shown in blue.

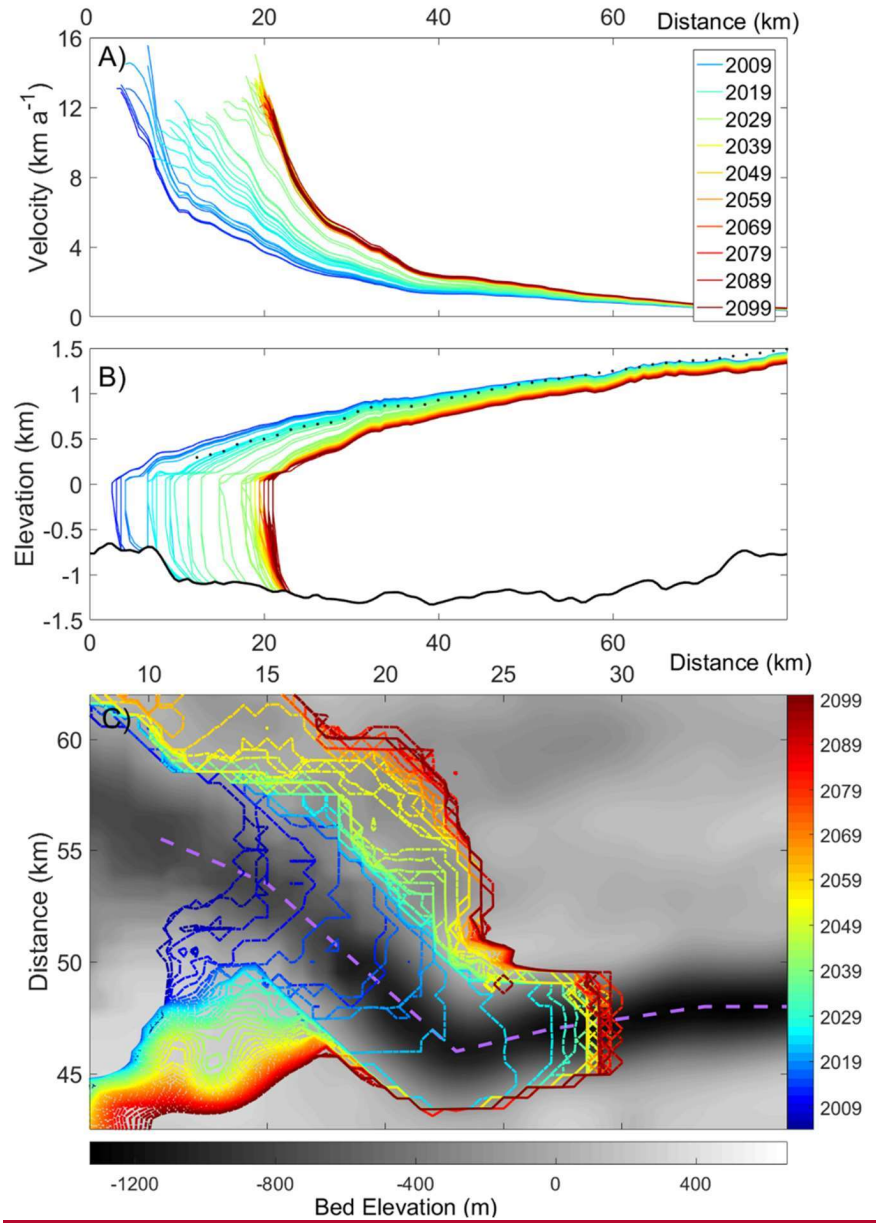

Figure 7. Modeled profiles of (A) January velocity and (B) January surface elevation along the center-flow-line (purple dash line in panel C) of Jakobshavn Isbræ from 2004 to 2099 for the RCP4.5 scenario. Bedrock elevation is shown in black. Black dotted line is the surface elevation profile extracted from radar data measured around 2010 (Gogineni et al., ~~2013~~2012). Profiles are shown at intervals of 1 years. Profiles are color-coded in the legend and range from blue to green and red. (C) Modeled July front positions (~~rainbow~~ color bar) over its bedrock (grayscale ~~color~~ bar)) at intervals of 2 years.

Under the RCP4.5 scenario (Fig. 6) surface runoff slowly rises over the 21st century, with RACMO simulating slightly greater runoff during the second half than for the first 50 years. Runoff increases

by 14% over the century. ~~Bottom o~~Ocean temperature at 300 m depth in the grid cell closest to Jacobshavn increases by 52%, and, as may be expected, has less variability than runoff.

Under this forcing, Jakobshavn Isbræ continues its retreat (Fig. 7) for 18 years after 2013, producing a total grounding line retreat of ~18 km upstream. As calving produces a steepening surface profile, terminus velocities increase, to reach a 21st century peak of ~19 km a^{-1} in 2031 summer. Eventually the calving front becomes higher than the crevasse penetration depth in the calving parameterization. This leads to a stable period with little inter-annual retreat and which lasts until the end of this century. During this period, nearly all of the seasonal retreats are offset by the following winter re-advances. Mass transport continually flattens and thins the ice geometry, leading to reduced flow speeds that eventually become half those of 2031, the 21st century peak.

The surprisingly high run-off anomaly in 2088 (Fig. 6) does not affect the stable state indicating run-off fluctuation alone cannot break this retreat pattern immediately. Once the inter-annual retreats cease in 2031, the dynamic thinning rate is greatly reduced because calving front height stops increasing.

Table 1 Estimates of glacier mass loss and grounding line retreat from different sources.

Source	Climate scenario	Mass loss 2004-2013 (10 years) (Gt)	Mass loss by 2100 (Gt)	Grounding line retreat 2004-2013 (km)	Grounding line retreat by 2100 (km)
This paper	RCP4.5	234	2068 (2044-2723)	7.0	18.5 (17.5-23.0)
Muresan et al. (2016)		220			
Nick et al. (~~2011~~2013)	A1B		1870 - 2281		14.0 - 26.0
Observations		225±15		7.0	

Table 1 shows estimates of glacier mass loss and retreat. Under RCP4.5, total cumulative mass change of Jakobshavn Isbræ is ~~2029~~2068 Gt by 2100, using best set of α, β and γ with ocean

temperature inputs from ensemble mean of 7 ESMs (Fig. 6). To estimate an upper bound for mass loss over this century, we scale the α parameter by 1.2 giving 2680 Gt for the same forcing (Fig. 8a). Using the HadGEM2-ES forcing, which is the same model used to force RACMO with α and γ set to their best estimates (Fig. 4) gives 2000 Gt. We suggest that this may be the lower reasonable bound of mass loss since the HadGEM-ES ocean temperatures rise notably slower than the ensemble mean (Fig. 6). Note that all 3 simulations of front position (Fig 7C, Fig. 8) show a relatively stable position around 18 km upstream from its 2013 location. Examination of the change in velocities during the simulation (Fig. 9) suggests that the explanation for this stability is strong flow convergence near the future glacier front that largely offsets dynamic thinning. Notice that the South side of the fast-flow-area in 20th century was quite close to ice-free land, while in later half of this century convergent flow in the South is fed by a substantial area of ice stream.

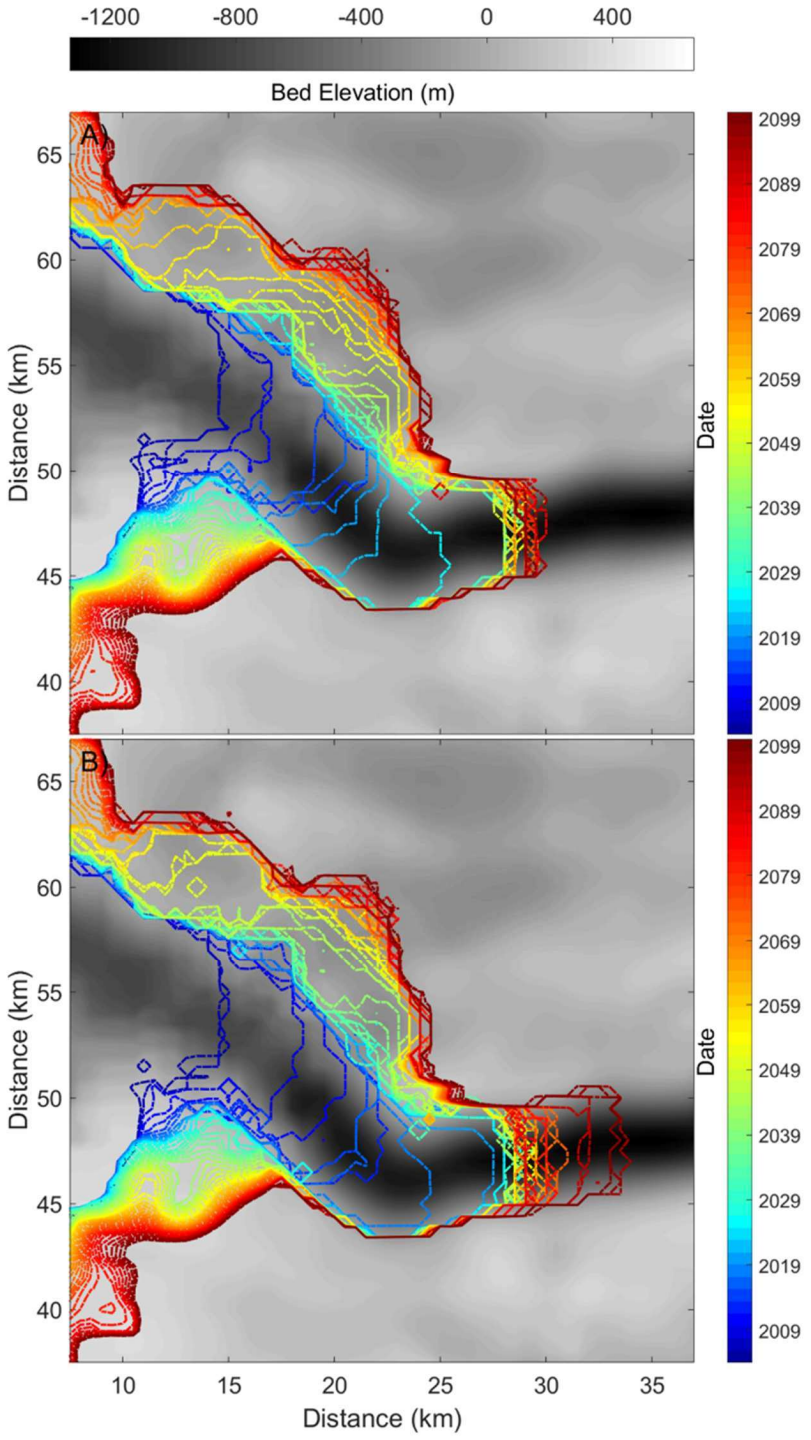

401

402 **Figure 8. Upper and lower estimates of July front positions within this century with colors**
403 **indicating the date (color bar) for A) lower bound with scalings of (1,0.8) and the HadGEM-ES**
404 **forcing B) upper bound of mass loss projection with (α, γ) parameter scalings of (1.2,1), and the**
405 **7-model ensemble climate forcing.**

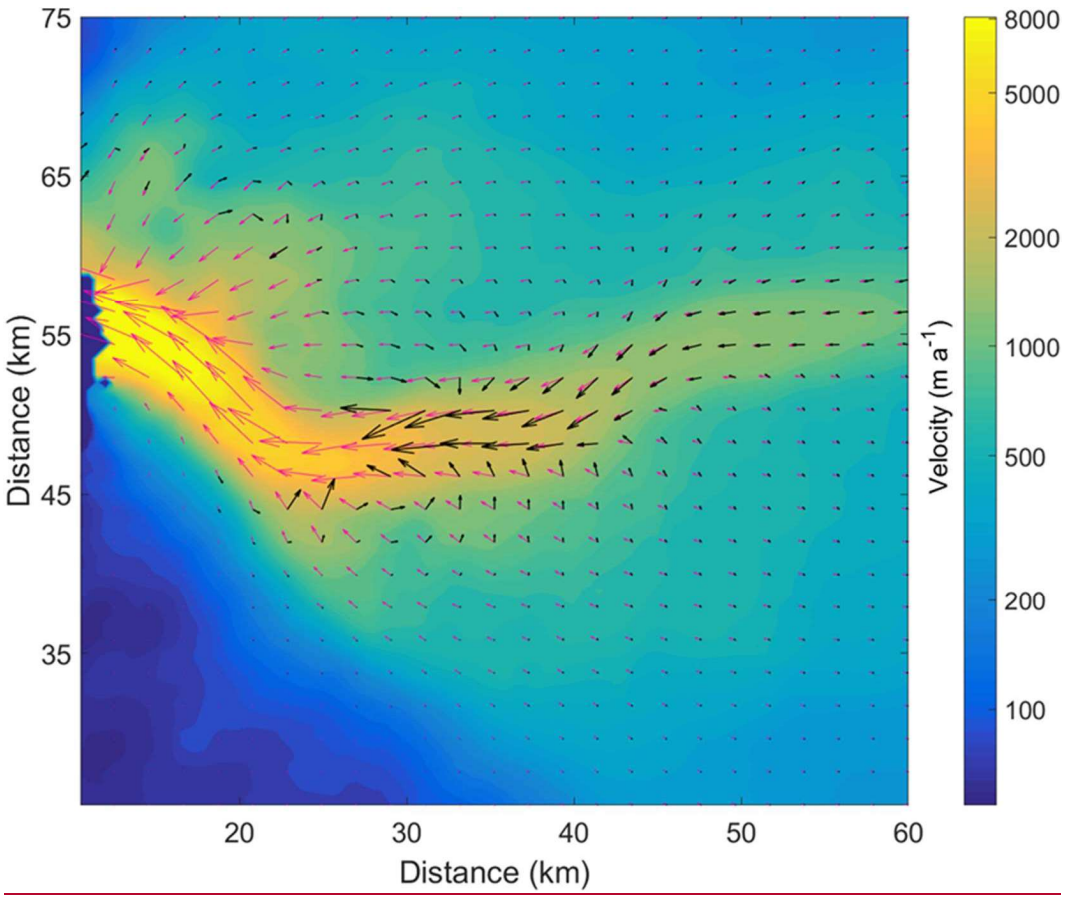

406

407

408 **Figure 9~~S6~~. Simulated velocity vectors in 2004 (pink vectors) with their magnitudes (right color**
409 **bar) and velocity difference between 2004 and 2099 (2099's minus 2004's, black vectors), for**
410 **clarity vector lengths are clipped ~~of vectors are limited that maximum length indicate magnitude~~**
411 **~~at>=~~ 5 km a^{-1}.**

412

413 Exploring the (α, γ) scaling parameter space we notice that values of (1.0, 0.8) produces a mass loss
414 over this century of 2021 Gt with the HadGEM-ES ocean forcing, almost the same value as for the
415 best set of parameters. This implies that less submarine melting (determined by γ) leads to larger ice
416 loss by dynamic processes. The reason is that lesser submarine melt allows a larger ice thickness at
417 the grounding line with stronger dynamic thinning in advancing season. Notice in our stress balance
418 equation (Eq. 3), thickness contributes to driving force term, thus ice flux across the grounding line
419 is highly nonlinear in ice thickness. This highly nonlinear relationship is also shown in our

sensitivity tests (Fig. 4). Over the mismatch field measured by front velocity (Fig. 4, Panel B), the velocity is partly dominated by low values of γ scaling around the scaling line for α = 1.06, while α is almost the only control on velocity over the region where scaled α<1.09. Within our sample space, the non-linear and non-monotonic relationship between submarine melting and retreats is clear (Fig. 4, Panel A). Around the point of scalings (α = 1.12, γ = 1.0), total retreat will increase no matter if γ is decreasing or increasing within the scaling range $0.8 < \gamma < 1.2$. The area where scaled $\alpha > 1.0$ in sample space is the very likely future condition for Jakobshavn Isbræ because increasing terminal ice cliff height caused by retreating into deep water will act as an amplifier to frontal driving force.

4 Discussion

4.1 Parameterization of Buttressing effect

The sudden 1.1°C rise in temperature of water entering Ilulissat fjord in 1997 (Holland et al., 2008) initiated rapid melting and disintegration of the floating ice mélange in 2003. This disintegration coincided with a near doubling of ice velocities. Modeling (Vieli et al., 2011) suggested that this was due to the reduction in buttressing from the floating ice-mélange. We can realistically reproduce the velocity variation of Jakobshavn Isbræ on seasonal and inter-annual scales using our parameterization of the buttressing effect from the ice mélange in the fjord.

Gladish et al. (2015) analyzed glacial flow speeds from 1998 to 2014, finding no correlation with Ilulissat fjord temperatures. This is because at the beginning of 2004, Jakobshavn's evolution entered a new phase with the disintegration of the ice mélange and floating ice shelf. We find good

correlations between Disko Bay temperatures and ice velocities from 2004 to 2014. The improvement in correlation with temperatures may be explained by a faster response between the grounded glacier and the fjord water temperatures after loss of the floating ice shelf. ~~Thus only freshly calved icebergs played roles in providing terminus resistance, and these could be reasonably supposed to react to seasonal fjord temperatures very quickly.~~

Buttressing would affect the calving process by altering the longitudinal resistive stress in the glacier. Temperatures in Ilulissat Fjord will be warmer during the 21st century under essentially all climate scenarios, even those with modest emissions, due to the thermal inertia of the oceans. Thus a new floating ice shelf is unlikely to form. Prior to 2004, there were large changes in Jakobshavn: loss of ~15 km long stiff ice mélange and the sudden rise in fjord temperatures in 1998. There are fewer mechanisms to effect such dramatic changes in the future now that almost the entirety of the glacier is grounded. We therefore propose that our representation of the mélange buttressing mechanism, tuned for 2004-2013, is likely to maintain its validity during the 21st century.

4.2 Horizontal shearing and viscosity

Van Der Veen et al. (2011) estimated a maximum horizontal shear stress of ~800 kPa across the shear margin of Jakobshavn Isbræ where the horizontal velocity shear reaches the peak, while the bed stress is only 10-40 kPa in fast flowing regions (Shapero et al., 2016). Given that the width of the Jakobshavn Isbræ fast flow region is typically under 5 km and its thickness is typically between 1-2 km, these numbers indicate that the shear margins provide at least an order of magnitude greater total resistance than the bed. Thus, the shear margin, rather than the bed of Jakobshavn Isbræ provides most of the resistance balancing the driving force. The main trunk of Jakobshavn Isbræ exhibits considerable seasonal velocity changes, while the slow moving ice outside the shear margin has little or no seasonal cycle. This flow structure implies speed gradients perpendicular to the flow

direction with large seasonal variation. These velocity shears would in turn generate large seasonal variations in effective ice viscosity (Eq. 6). This mechanism ~~is due to the non-linear rheology of the ice~~ is due to the non-linear rheology of the ice in the fast flow region: increases in the speed of fast flowing ice cause increases in horizontal shear stress across the margins, reduced viscosity, and further increased horizontal velocity shear, allowing further increase to speeds in the fast flow region. Observations show that, as the terminus retreated into deeper water, seasonal fluctuations in terminus velocity increased (Joughin et al. 2008). By 2012, the summer time peak terminus velocity was ~ 17 km a^{-1}, more than twice the wintertime minimum velocity (Joughin et al. 2014). This amplified seasonal velocity cycle was likely enhanced by the shear-margin weakening mechanism.

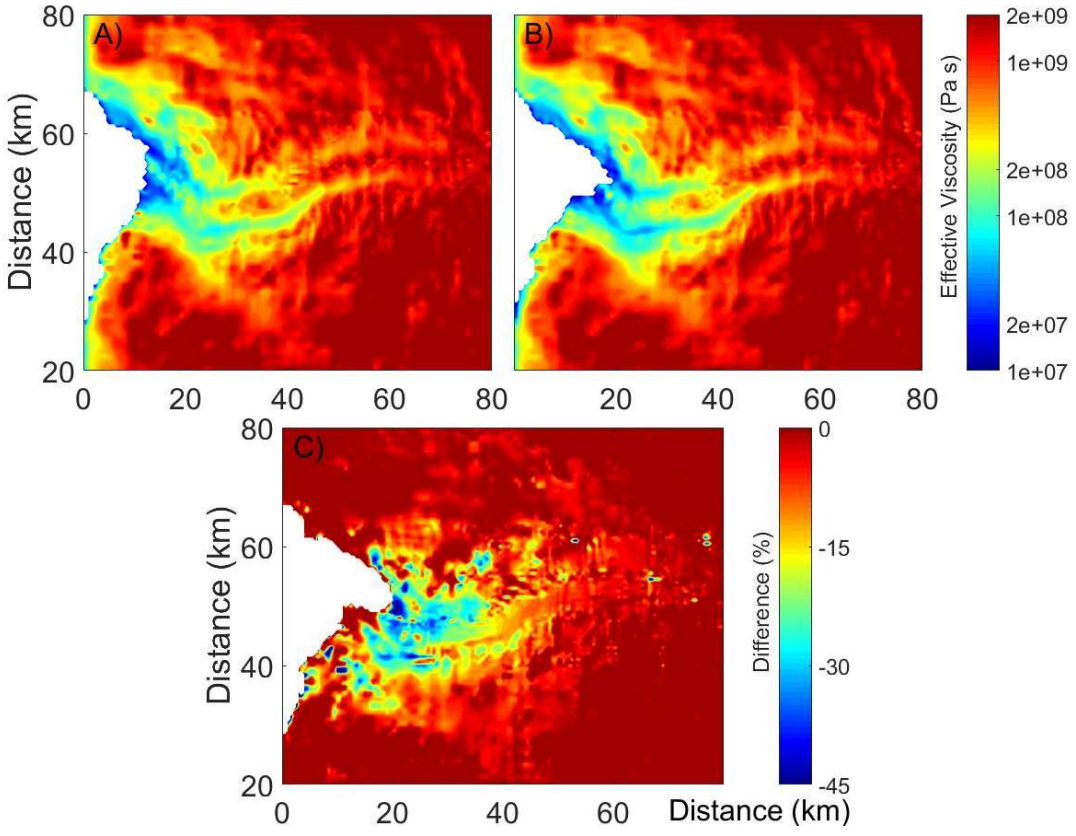

Figure 10~~8~~. Modeled annual mean of vertically averaged effective viscosity $\Phi\mu$ (Eq. 5) in 2004 (A) and 2013 (B) and the percentage decreases from 2004 to 2013 (C).

Our modeled shear margin weakening on decadal scales is consistent with other estimates from a thermomechanical ice flow model of Jakobshavn Isbræ forced by calving front positions (Bondzio et al., 2017). Their modeled viscosity drops between 2003 to 2015 reach ~ 40% which is close to our maximum viscosity decrease of ~ 45% between 2004 to 2013 (Fig. ~~8~~10). The extreme calving season we simulated in summer 2012 was accompanied by ~ 12 km a^{-1} variations in speed at the calving front, which were facilitated by the accompanying shear margin-induced ice viscosity reductions of 60% at the time of maximum terminus advance. Simpler models of Jakobshavn Isbræ, using a flowband model (Nick et al., ~~2011~~2013) or simple calving parameterizations with no seasonal cycle (Muresan et al., 2016) cannot produce these seasonal variations in shearing. However, our model accommodates both the seasonal forcing from calving and the three-dimensional seasonal velocity shear impacts on effective viscosity. Without this physical process, speedups during intense calving events would be under-estimated, and this would lead to under-estimated mass transportation during the retreat. Bondzio et al. (2017) used a thermomechanical ice flow model to evolve the ice viscosity, which depends on a damage parameter that softens the ice in the shear margins. But their damage parameter also stays constant in time. Thus both the models of Bondzio et al., (2017) and ours only consider the contribution from strain rate weakening in time to evolving viscosity. Thermodynamics could play some role in changing viscosity, presumably if the ice temperatures increased over time, but our temperatures are fixed at -10°C.

Several ~~absent processes in~~ processes absent from our model could affect ice viscosity. Crevasses saturated by surface melt water within the shear margins of Jakobshavn are visible on satellite images (Lampkin et al., 2013).~~,occurred and last in summer that are visible on satellite images (Lampkin et al., 2013).~~ This~~ese~~ melt water can transfer heat throughout the ice column through discharge within crevasses and moulins thus softening the ice (Phillips et al., 2010). ~~Consideration~~ ~~a~~Incorporating a continuum damage model in BISICLES would further exaggerate the shear margin

weakening as it raises the non-linear dependence of strain rates ~~to~~on stress fields (Sun et al., 2017).

4.3 Comparison with previous estimates

The cumulative mass change of Jakobshavn Isbræ estimated from airborne and satellite laser altimetry for 1997–2014 was tabulated Muresan et al. (2016). The mass loss over the 10-year period 2004-2013 modeled by Muresan et al. (2016) is closer to observations than ours (Table 1). This is partly due to different tuning targets: matching observed mass change was a stated target in their study, whereas our study targets ice front position and velocity. Their close match to observed mass loss may be partly due to cancelling errors: 1) their modeled calving front barely moves after 2006, which leads to under-estimation of mass change; and 2) the modeled fast flow widths are larger than observations, which amplifies the mass flux across the calving front. These two biases will not always offset each other perfectly in the future.

Muresan et al. (2016) failed to simulate the retreat of Jakobshavn Isbræ after 2010. This may be due to the thickness threshold employed in their calving parameterization. Once Jakobshavn Isbræ terminus has retreated into the deeper part of the bedrock trough, the terminus height might never drop below their calving threshold of 375 m. In this case their calving rate will be solely due to the eigen parameterization of strain rates. Moreover, absence of seasonality in their calving front leads to under-estimated dynamic thinning, which is a key prerequisite for further calving. In contrast, our crevasse-depth calving model depends on stresses and surface water run-off with strong seasonal variation. As the terminus retreats and the surface slope steepens the enhanced surface stretching enhances the opening of crevasses in both calving parameterizations.

Nick et al. (~~2011~~2013) used a flow-band model to estimate a mass loss of 2280 Gt for Jakobshavn Isbræ by 2100 under the A1B climate scenario (Table 1). In our model we use RCP4.5 climate

forcing, which has lower temperature rises than A1B, especially after 2050. Nick et al. (~~2011~~2013) prescribed a flow-band that has a near uniform width of 5 km near the terminus. Later modeling work using a similar model suggested that stability of the glacier is fundamentally controlled by geometry, and in reality the width varies along the ice-stream (Steiger et al. 2017). Nick et al. (~~2011~~2013) chose sets of parameters that produced small inter-annual retreats of Jakobshavn from 2000-2010, which may limit mass loss and retreat. The absence of the shear margin weakening feedback in their model also likely causes underestimation of mass loss. This could account for the comparable projected mass loss to our results, and less terminus retreat (Table 1), even though their climate forcing scenario was warmer.

Another SSA model (Bondzio et al., 2018) projects larger retreats than ours, and ~~with~~uses a calving parameterization that predicts the location of calving dependsing on tensile stress distribution, regardless of ice thickness. Their calving criterion implies a nonlinear relationship between crevasse depth and stress, ~~C~~compared~~ing~~ with our linear dependence~~physics-based formula for crevasse depth~~ (Eq. 12)~~., their calving criterion implies a nonlinear relationship between crevasse depth and stress,~~ We suggest that this nonlinearity ~~which~~ might leads to overestimated retreats.

4.4 Model improvements

We overestimate mass loss relative to observations over Jakobshavn Isbræ drainage basin for 2004-2013 (Table 1). ~~The~~ One ~~main~~ reason ~~is excessive~~~~could be the~~for the discrepancy may be errors in ~~between our~~ initial ice thickness and real geometry in 2004. Excessive dynamic thinning was simulated over the lowest ~ 20 km of the main trunk due to over-estimated summer speed. For example, modeled front velocity soared to a peak of ~ 20 km a^{-1} in summer 2012, while the observed maximum speed is only 18 km a^{-1} (Joughin et al., 2014). In this summer, we simulated a series of full-thickness calving events that eventually left an unprecedented tall ice cliff. In reality, calving

events do not always occur to full thickness, thus the glacier tends to form a shorter ice cliff that caters for lower velocity and less dynamic thinning.

Since the grounding line of Jakobshavn retreated to the bottom of a reverse bed slope in 2009, the height of the calving front has generally increased, causing larger mass flux downstream across the calving front. Instead of enhancing the seasonal fluctuation of calving front position, substantial winter calving events have occurred instead. Given the fact that these calving events have reduced the typical winter advance from ~ 6 km to ~ 3 km since 2010, winter calving is now likely as important as summer run-off-driven calving. During this period of low magnitude seasonal fluctuations, a series of retreats gradually moved the calving front position on inter-annual scale. In contrast, the inter-annual retreats before 2009 were mostly driven by single calving seasons, e.g., May to July 2009. Our model using the Benn calving model is better able to ~~stimulate~~simulate this earlier retreat pattern, which is largely determined by each year's peak surface water run-off.

The grounding line of Jakobshavn Isbræ is unlikely to return to shallow water in the remainder of the 21st century because bedrock elevations < - 1000 m beneath the main trunk further extend a further ~ 60 km inland. Accordingly, the latest retreat pattern including winter calving, is likely closer to the pattern of future evolution of Jakobshavn Isbræ. A short floating part due to winter calving is always accompanied by weaker lateral drag and steeper surface slope near the grounding line, all of which are conducive for faster ice-flow. So, winter calving would enhance the downstream mass transportation, a missing process in our model.

The process of winter calving must take place without any surface water. That calving must be generated by processes affecting ice ~~cliff~~front stability, and that is likely due to changes at the base rather than the surface. Evidence of calving by opening of basal crevasses and splitting comes from terrestrial radar showing the terminus lifting several days prior to a large calving (Xie et al., 2016;

James et al., 2014). These observations suggest that the glacier is not in hydrostatic equilibrium during calving. Our simulation specifies the glacier is in hydrostatic equilibrium on timescales of the simulation. Our model cannot simulate the process of up-lifting. Instead we assume the upper and lower surface would instantly lift to the state of floating (Eq. 1). However, there is some evidence that Jakobshavn must behave super-buoyantly in winter. We observe that the simulated grounding line of Jakobshavn retreats even after cessation of calving front retreat (Fig. 3). These retreats can be explained by rapid dynamic thinning near the grounding line leading to its buoyancy exceeding gravity and, consequently, floating. Winter calving can occur in later winter (Cassotto et al., 2015) when calving front height is at its annual minimum and presumably at its least vulnerable to structural failure. Hence, MICI (Marine Ice Cliff Instability) cannot explain this type of calving, and winter calving is specifically excluded from parametrizations of MICI (Pollard et al., 2018). The existence of winter calving has greatly reduced the range of seasonal fluctuations in front position, which inhibited the growing of a temporary ice shelf that would buttress the grounded ice. Thus, lack of winter calving would cause underestimation of dynamic thinning as the glacier grows in winter.

A combination of discrete element model and continuum ice-dynamic model (solving the 3-Dimensional full-stokes equation) is able to reliably replicate observed calving styles in the case of a super-buoyant terminus (Benn et al. 2017). The discrete element model allows investigation of calving processes in unprecedented detail by analyzing the stress pattern dominated by glacier geometry and boundary conditions. However, these calving processes are beyond the capability of a calving parameterization based on surface crevasse depth assuming depth-independent flow. Better understanding of this buoyancy-driven calving and further model development to represent

more details such as fracture propagation are needed to accurately simulate glacier's future evolution.

Ice thickness and basal topography with resolution of 150 m became available for main outlet glaciers of Greenland (Morlighem et al., 2017) recently (Fig. S3). This ~~allows~~eases finer mesh resolution to be used for~~in~~ modeling ~~works~~ which then might~~would~~ ~~be expected to~~ reveal more details of ice-stream behavior especially ~~on~~ perpendicular-to-flow direction, including more precise shear-margin-weakening and ~~single~~ calving near side walls. Our assumption of simple Weertman ~~Other than our simple assumption of~~ basal drag (Eq. 7) may be improved by~~,~~ implementing a physics-based basal sliding law (Schoof, 2010; Gagliardini et al., 2014; Tsai et al., 2015), although basal drag accounts for only about 2% of present-day buttressing (Shapero et al., 2016). ~~–~~An improved sliding relation would likely produce more speedup and retreats in model results as dynamic thinning ~~constantly~~ can reduce the effective pressure~~,~~ ~~which~~ leads~~ing~~ to lower basal shear stress.

5 Conclusion

We use a three-dimensional dynamic ice-sheet model with a physically-based calving parameterization to model the evolution of Jakobshavn Isbræ. After tuning the parameters, our model can accurately reproduce Jakobshavn Isbræ's retreats and velocity changes from 2004-2013 on both seasonal and inter-annual scale. We project Jakobshavn Isbræ's future dynamic changes with climate forcing data from RACMO (2014-2099) and an ensemble mean of 7 Earth System Models for the RCP4.5 scenario.

We successfully model two-dimensional ice~~-flow patterns~~ velocity and viscosity structures and their seasonal variations for Jakobshavn Isbræ, which are missing from several previous modeling studies.

Moreover, capturing these two-dimensional ~~patterns~~structures allows us to handle the influence of horizontal velocity shear on effective ice viscosity, which impacts on speedup processes of Jakobshavn Isbræ.~~–~~

Over most of the 21st century, Jakobshavn Isbræ's grounding line will, we predict, retreat along the deep parts of a basal trough where bedrock elevation is significantly lower than at the present grounding line. Retreat slows as the front reaches the deepest parts of the trough, but by the end of the century acceleration is possible as the front passes that position. Using the current generation of calving parameterizations, which are essentially thickness threshold models, is challenging because of the increasing height of the calving front as Jakobshavn Isbræ retreats, meaning that crevasse penetration depths become too small to initiate calving. Our model successfully reproduced Jakobshavn Isbræ's retreat down a reverse bed slope with an elevation drop of ~ 400 m and the subsequent temporarily stable calving front position in 2013 and 2014.

Our results suggest that rapid dynamic thinning and calving caused by deep crevasse penetration are responsible for most of its recent mass loss, and will be ~~a~~ decisive processes in future mass loss. Further exploration of the physics of calving and basal sliding of Greenland outlet glaciers are required to improve future projections.

Acknowledgements

This study is supported by National Key Science Program for Global Change Research (2015CB953601), National Key Research and Development Program of China (2018YFC1406104) and National Natural Science Foundation of China (No. 41506212). We thank Stephen Cornford for his help in implementing some parameterizations used in our model. Three referees provided very helpful suggestions on the model results. Rupert Gladstone is supported by Academy of Finland grant number 286587.

References

Alexander, P. M., and Luthcke, S. B.: Greenland Ice Sheet seasonal and spatial mass variability from model simulations and GRACE (2003-2012), The Cryosphere, 10(3), 1259, 2016.

Amundson, J. M., Fahnestock, M., Truffer, M., Brown, J., Lüthi, M. P., and Motyka, R. J.: Ice mélange dynamics and implications for terminus stability, Jakobshavn Isbræ, Greenland, J. Geophys. Res.-Earth Surf., 115(F1), 2010.

Bamber, J. L., Layberry, R. L., and Gogineni, S. P.: A new ice thickness and bed data set for the Greenland ice sheet: 1. Measurement, data reduction, and errors, J. Geophys Res.-Atmos, 106(D24), 33773-33780, 2001.

Benn, D. I., Åström, J., Zwinger, T., Todd, J., Nick, F. M., Cook, S., Hulton, N. R.J., and Luckman, A.: Melt-under-cutting and buoyancy-driven calving from tidewater glaciers: new insights from discrete element and continuum model simulations, J. Glaciol., 63(240), 691-702, 2017.

Benn, D. I., Warren, C. R., and Mottram, R. H.: Calving processes and the dynamics of calving glaciers, Earth-Sci Rev., 82(3), 143-179, 2007.

Bentsen, M., Bethke, I., Debernard, J. B., Iversen, T., Kirkevåg, A., Seland, Ø., Drange, H., Roelandt, C., Seierstad, I. A., Hoose, C., and Kristjánsson, J. E.: The Norwegian earth system model, NorESM1-M-Part 1: Description and basic evaluation, Geosci. Model Dev., 5, 2843-2931, 2012.

Block, A. E., and Bell, R. E.: Geophysical evidence for soft bed sliding at Jakobshavn Isbrae, West Greenland, The Cryosphere Discussions, 5, 339-366, 2011.

Bondzio, J. H., Morlighem, M., Seroussi, H., Kleiner, T., Rückamp, M., Mouginot, J., Moon, T., Larour, E. Y., and Humbert, A.: The mechanisms behind Jakobshavn Isbræ's acceleration and mass loss: A 3-D thermomechanical model study, Geophys. Res. Lett., 44(12), 6252-6260, 2017.

Bondzio, J. H., Morlighem, M., Seroussi, H., Wood, M. H., and Mouginot, J.: Control of ocean temperature on Jakobshavn Isbræ's present and future mass loss, Geophys. Res. Lett., 45(23), 12-912, 2018.

Cassotto, R., Fahnestock, M., Amundson, J. M., Truffer, M., and Joughin, I.: Seasonal and interannual variations in ice mélange and its impact on terminus stability, Jakobshavn Isbrae, Greenland, J. Glaciol., 61(225), 76-88, 2015.

Collins, W. J., Bellouin, N., Doutriaux-Boucher, M., Gedney, N., Halloran, P., Hinton, T., Hughes, J., Jones, C. D., Joshi, M., Liddicoat, S., Martin, G., O'Connor, F., Rae, J., Senior, C., Sitch, S., Totterdell, I., Wiltshire, A., and Martin, G.: Development and evaluation of an Earth-System model HadGEM2, Geosci. Model Dev., 4(4), 1051-1075, 2011.

Cornford, S. L., Martin, D. F., Graves, D. T., Ranken, D. F., Le Brocq, A. M., Gladstone, R. M., Payne, A., J., Ng, E. G., and Lipscomb, W. H.: Adaptive mesh, finite volume modeling of marine ice sheets, J. Comput. Phys., 232(1), 529-549, 2013.

Cornford, S. L., Martin, D. F., Payne, A. J., Ng, E. G., Le Brocq, A. M., Gladstone, R. M., Edwards, T. L., Shannon, S. R., Agosta, C., Van Den Broeke, M. R., Hellmer, H. H., Krinner, G., Ligtenberg, S. R. M., Timmermann, R., and Hellmer, H. H.: Century-scale simulations of the response of the

West Antarctic Ice Sheet to a warming climate, The Cryosphere, 9, 1-22, 2015.

Cowton, T. R., Sole, A. J., Nienow, P. W., Slater, D. A., and Christoffersen, P.: Linear response of east Greenland's tidewater glaciers to ocean/atmosphere warming, P. Natl. Acad. Sci. USA, 115(31), 7907-7912, 2018.

Csatho, B., Schenk, T., Van Der Veen, C. J., and Krabill, W. B.: Intermittent thinning of Jakobshavn Isbrae, West Greenland, since the little ice age, J. Glaciol., 54(184), 131-144, 2008.

Cuffey, K. M., and Paterson, W. S. B.: The physics of glaciers. Academic Press, 2010.

Dee, D., Uppala, S., Simmons, A., Berrisford, P., Poli, P., Kobayashi, S., Andrae, U., Balmaseda, M., Balsamo, G., Bauer, P., Bechtold, P., Beljaars, A. C. M., van de Berg, L., Bidlot, J., Bormann, N., Delsol, C., Dragani, R., Fuentes, M., Geer, A. J., Haimberger, L., Healy, S. B., Hersbach, H., Hólm, E. V., Isaksen, L., Kållberg, P., Köhler, M., Matricardi, M., McNally, A. P., Monge-Sanz, B. M., Morcrette, J. J., Park, B. K., Peubey, C., de Rosnay, P., Tavolato, C., Thépaut, J. N., and Vitart, F.: The ERA-Interim reanalysis: Configuration and performance of the data assimilation system, Q. J. Roy. Meteor. Soc., 137, 553–597, 2011.

Dufresne, J. L., Foujols, M. A., Denvil, S., Caubel, A., Marti, O., Aumont, O., Balkanski, Y., Bekki, S., Bellenger, H., Benshila, R., Bony, S., Bopp, L., Braconnot, P., Brockmann, P., Cadule, P., Cheruy, F., Codron, F., Cozic, A., Cugnet, D., De Noblet, N., Duvel, J. P., Eth´e, C., Fairhead, L., Fichefet, T., Flavoni, S., Friedlingstein, P., Grandpeix, J. Y., Guez, L., Guilyardi, E., Hauglustaine, D., Hourdin, F., Idelkadi, A., Ghattas, J., Joussaume, S., Kageyama, M., Krinner, G., Labetoulle, S., Lahellec, A., Lefebvre, M. P., Lefevre, F., Levy, C., Li, Z. X., Lloyd, J., Lott, F., Madec, G., Mancip, M., Marchand, M., Masson, S., Meurdesoif, Y., Mignot, J., Musat, I., Parouty, S., Polcher, J., Rio, C., Schulz, M., Swingedouw, D., Szopa, S., Talandier, C., Terray, P., Viovy, N., and Bony, S.: Climate change projections using the IPSL-CM5 Earth System Model: from CMIP3 to CMIP5, Clim. Dynam., 40(9-10), 2123-2165, 2013.

Gagliardini, O., Passalacqua, O., and Werder, M. A.: Retroactions between Basal Hydrology and Basal Sliding from Numerical Experiments. In AGU Fall Meeting Abstracts, 2014.

Giorgetta, M. A., Jungclaus, J., Reick, C. H., Legutke, S., Bader, J., Böttinger, M., Brovkin, V., Crueger, T., Esch, M., Fieg, K., Glushak, K., Gayler, V., Haak, H., Hollweg, H., Ilyina, T., Kinne, S., Kornblueh, L., Matei, D., Mauritsen, T., Mikolajewicz, U., Mueller, W., Notz, D., Pithan, F., Raddatz, T., Rast, S., Redler, R., Roeckner, E., Schmidt, H., Schnur, R., Segschneider, J., Six, Katharina D., Stockhause, M., Timmreck, C., Wegner, J., Widmann, H., Wieners, K., Claussen, M., Marotzke, J., Stevens, B., and Glushak, K.: Climate and carbon cycle changes from 1850 to 2100 in MPI-ESM simulations for the Coupled Model Intercomparison Project phase 5, J. Adv. Model Earth Sy., 5(3), 572-597, 2013.

Gladish, C. V., Holland, D. M., Rosing-Asvid, A., Behrens, J. W., and Boje, J.: Oceanic boundary conditions for Jakobshavn Glacier. Part I: Variability and renewal of Ilulissat Icefjord waters, 2001-14, J. Phys. Oceanogr., 45(1), 3-32, 2015.

Gogineni, P.: CReSIS radar depth sounder data, Center for Remote Sensing of Ice Sheets, Lawrence, KS https://data.cresis.ku.edu, 2012.

Gordon, H. B., Rotstayn, L. D., McGregor, J. L., Dix, M. R., Kowalczyk, E. A., O'Farrell, S. P., Waterman, L. J., Hirst, A. C., Wilson, S. G., Collier, M. A., and Watterson, I. G.: The CSIRO Mk3 climate system model, 2002.

Habermann, M., Truffer, M., and Maxwell, D.: Changing basal conditions during the speed-up of Jakobshavn Isbræ, Greenland, The Cryosphere, 7(6), 1679-1692, 2013.

Holland, D. M., Thomas, R. H., De Young, B., Ribergaard, M. H., and Lyberth, B.: Acceleration of Jakobshavn Isbrae triggered by warm subsurface ocean waters, Nat. Geosci., 1(10), 659, 2008.

Howat, I. M., Ahn, Y., Joughin, I., van den Broeke, M. R., Lenaerts, J. T., and Smith, B.: Mass balance of Greenland's three largest outlet glaciers, 2000-2010, Geophys. Res. Lett., 38(12), 2011.

Jakobsson, M., Mayer, L., Coakley, B., Dowdeswell, J. A., Forbes, S., Fridman, B., Hodnesdal, H., Noormets, R., Pedersen, R., Rebesco, M., Schenke, H. W., Zarayskaya, Y., Accettella, D., Armstrong, A., Anderson, R. M., Bienhoff, P., Camerlenghi, A., Church, I., Edwards, M., Gardner, J. V., Hall, J. K., Hell, B., Hestvik, O., Kristoffersen, Y., Marcussen, C., Mohammad, R., Mosher, D., Nghiem, S. V., Pedrosa, M. T., Travaglini, P. G., and Schenke, H. W.: The international bathymetric chart of the Arctic Ocean (IBCAO) version 3.0, Geophys. Res. Lett., 39(12), 2012.

James, T. D., Murray, T., Selmes, N., Scharrer, K., and O'Leary, M.: Buoyant flexure and basal crevassing in dynamic mass loss at Helheim Glacier, Nat. Geosci., 7(8), 593-596, 2014.

Ji, D., Wang, L., Feng, J., Wu, Q., Cheng, H., Zhang, Q., Yang, J., Dong, W., Dai, Y., Gong, D., Zhang, R., Wang, X., Liu, J., Moore, J. C., Chen, D., and Zhang, R. H.: Description and basic evaluation of Beijing Normal University Earth system model (BNU-ESM) version 1, Geosci. Model Dev., 7(5), 2039-2064, 2014.

Joughin, I., Abdalati, W., and Fahnestock, M.: Large fluctuations in speed on Greenland's Jakobshavn Isbrae glacier. Nature, 432(7017), 608, 2004.

Joughin, I., Howat, I. M., Fahnestock, M., Smith, B., Krabill, W., Alley, R. B., Stern, H., and Truffer, M.: Continued evolution of Jakobshavn Isbrae following its rapid speedup, J. Geophys. Res.-Earth Surf., 113(F4), 2008.

Joughin, I., Smith, B. E., and Howat, I. M.: A complete map of Greenland ice velocity derived from satellite data collected over 20 years, J. Glaciol., 64(243), 1-11, 2018.

Joughin, I., Smith, B. E., Howat, I. M., Scambos, T., and Moon, T.: Greenland flow variability from ice-sheet-wide velocity mapping, J. Glaciol., 56(197), 415-430, 2010.

Joughin, I., Smith, B., Shean, D., and Floricioiu, D.: Brief communication: Further summer speedup of Jakobshavn Isbræ, The Cryosphere, 8, 209-214, 2014.

Krabill, W., Abdalati, W., Frederick, E., Manizade, S., Martin, C., Sonntag, J., Swift, R., Thomas, R., Wright, W., and Yungel, J.: Greenland ice sheet: High-elevation balance and peripheral thinning. Science, 289(5478), 428-430, 2000.

Lampkin, D. J., Amador, N., Parizek, B. R., Farness, K., and Jezek, K.: Drainage from water-filled crevasses along the margins of Jakobshavn Isbræ: A potential catalyst for catchment expansion, J. Geophys. Res.-Earth Surf., 118(2), 795-813, 2013.

Luckman, A., and Murray, T.: Seasonal variation in velocity before retreat of Jakobshavn Isbræ, Greenland, Geophys. Res. Lett., 32(8), 2005.

Morlighem, M., Williams, C. N., Rignot, E., An, L., Arndt, J. E., Bamber, J. L., Catania, G., Chauché, N., Dowdeswell, J. A., Dorschel, B., Fenty, I., Hogan, K., Howat, I., Hubbard, A., Jakobsson, M.,

Jordan, T. M., Kjeldsen, K. K., Millan, R., Mayer, L., Mouginot, J., Noël, B. P. Y., O'Cofaigh, C., Palmer, S., Rysgaard, S., Seroussi, H., Siegert, M. J., Slabon, P., Straneo, F., Van den Broeke, M. R., Weinrebe, W., Wood, M., and Zinglersen, K. B.: BedMachine v3: Complete bed topography and ocean bathymetry mapping of Greenland from multibeam echo sounding combined with mass conservation, Geophys. Res. Lett., 44(21), 11-051, 2017.

Moss, R. H., Edmonds, J. A., Hibbard, K. A., Manning, M. R., Rose, S. K., Van Vuuren, D. P., Carter, T. R., Emori, S., Kainuma, M., Kram, T., Meehl, G. A., Mitchell, J. F.B., Nakicenovic, N., Riahi, K., Smith, S. J., Stouffer, R. J., Thomson, A. M., Weyant, J. P., and Wilbanks, T. J.: The next generation of scenarios for climate change research and assessment. Nature, 463(7282), 747-756, 2010.

Motyka, R. J., Truffer, M., Fahnestock, M., Mortensen, J., Rysgaard, S., and Howat, I.: Submarine melting of the 1985 Jakobshavn Isbræ floating mélange and the triggering of the current retreat, J. Geophys. Res.-Earth Surf., 116(F1), 2011.

Muresan, I. S., Khan, S. A., Aschwanden, A., Khroulev, C., Van Dam, T., Bamber, J., Van Den Broeke, M. R., Wouters, B., Munneke, P. K., and Kjær, K. H.: Modelled glacier dynamics over the last quarter of a century at Jakobshavn Isbræ, The Cryosphere, 10(2), 597-611, 2016.

Nick, F. M., Vieli, A., Andersen, M. L., Joughin, I., Payne, A., Edwards, T. L., Pattyn, F. and van de Wal, R. S.: Future sea-level rise from Greenland's main outlet glaciers in a warming climate. Nature, 497(7448), 235, 2013.

Phillips, T., Rajaram, H., & Steffen, K.: Cryo-hydrologic warming: A potential mechanism for rapid thermal response of ice sheets, Geophys. Res. Lett., 37(20), 2010.

Pollard, D., and DeConto, R. M.: Description of a hybrid ice sheet-shelf model, and application to Antarctica, Geosci. Model Dev., 5(5), 1273, 2012.

Pollard, D., DeConto, R. M and Alley, R. B.: A continuum model (PSUMEL1) of ice mélange and its role during retreat of the Antarctic Ice Sheet, Geosci. Model Dev., 11, 5149-5172, 2018.

Schoof, C., and Hindmarsh, R. C.: Thin-film flows with wall slip: an asymptotic analysis of higher order glacier flow models, Q. J. Mech. Appl. Math., 63(1), 73-114, 2010.

Shapero, D. R., Joughin, I. R., Poinar, K., Morlighem, M., and Gillet-Chaulet, F.: Basal resistance for three of the largest Greenland outlet glaciers, J. Geophys. Res.-Earth Surf., 121(1), 168-180, 2016.

Sohn, H. G., Jezek, K. C., and van der Veen, C. J.: Jakobshavn Glacier, West Greenland: 30 years of spaceborne observations, Geophys. Res. Lett., 25(14), 2699-2702, 1998.

Steiger, N., Nisancioglu, K. H., Åkesson, H., Fleurian, B. D., and Nick, F. M.: Simulated retreat of Jakobshavn Isbræ since the Little Ice Age controlled by geometry, The Cryosphere, 12(7), 2249-2266, 2018.

Sun, S., Cornford, S. L., Moore, J. C., Gladstone, R., & Zhao, L.: Ice shelf fracture parameterization in an ice sheet model, The Cryosphere, 11(6), 2543-2554, 2017.

Tsai, V. C., Stewart, A. L., and Thompson, A. F.: Marine ice-sheet profiles and stability under

Coulomb basal conditions, J. Glaciol., 61(226), 205-215, 2015.

Van Angelen, J. H., M Lenaerts, J. T., Van den Broeke, M. R., Fettweis, X., and Meijgaard, E.: Rapid loss of firn pore space accelerates 21st century Greenland mass loss, Geophys. Res. Lett., 40(10), 2109-2113, 2013.

Van Der Veen, C. J., Plummer, J. C., and Stearns, L. A.: Controls on the recent speed-up of Jakobshavn Isbræ, West Greenland, J. Glaciol., 57(204), 770-782, 2011.

Vieli, A., and Nick, F. M.: Understanding and modelling rapid dynamic changes of tidewater outlet glaciers: issues and implications, Surv. Geophys., 32(4-5), 437-458, 2011.

Watanabe, S., Hajima, T., Sudo, K., Nagashima, T., Takemura, T., Okajima, H., Nozawa, T., Kawase, H., Abe, M., Yokohata, T., Ise, T., Sato, H., Kato. E., Takata, K., Emori, S., and Kawamiya, M.: MIROC-ESM 2010: Model description and basic results of CMIP5-20c3m experiments, Geosci. Model Dev., 4(4), 845, 2011.

Weertman, J. ~~1957~~: On the Sliding of Glaciers~~.~~, J. Glaciol., 3(21), 33-38, 1957.

Xie, S., Dixon, T. H., Voytenko, D., Holland, D. M., Holland, D., and Zheng, T.: Precursor motion to iceberg calving at Jakobshavn Isbræ, Greenland, observed with terrestrial radar interferometry, J. Glaciol., 62(236), 1134-1142, 2016.

Supplementary information

Simulated retreat of Jakobshavn Isbræ during the 21st century

Guo et al.

Correspondence to: X. Guo (xiaoran.guo@foxmail.com)

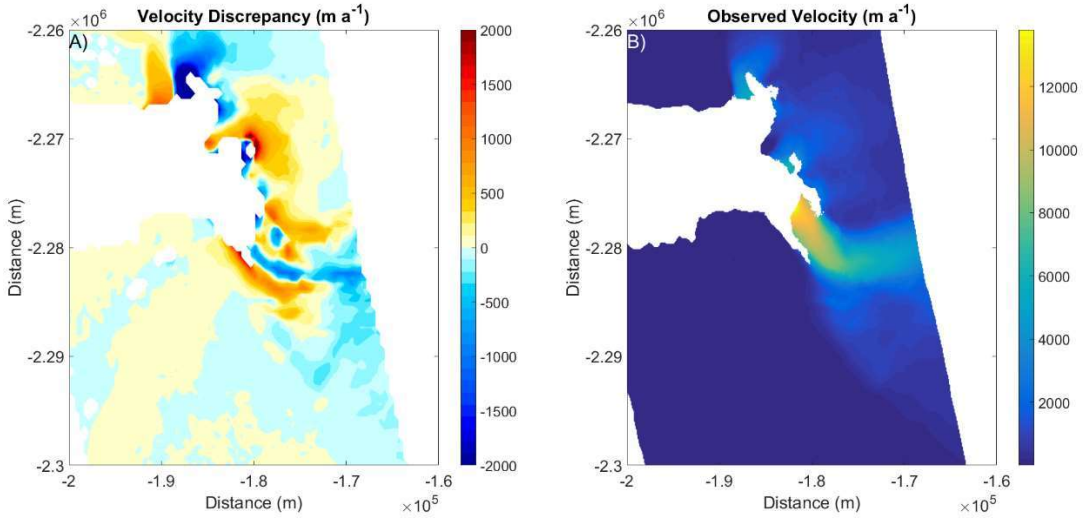

Figure S21. A) Velocity discrepancy (velocity from inversion - observed) and B) the observed velocity field (Joughin et al., 2010).

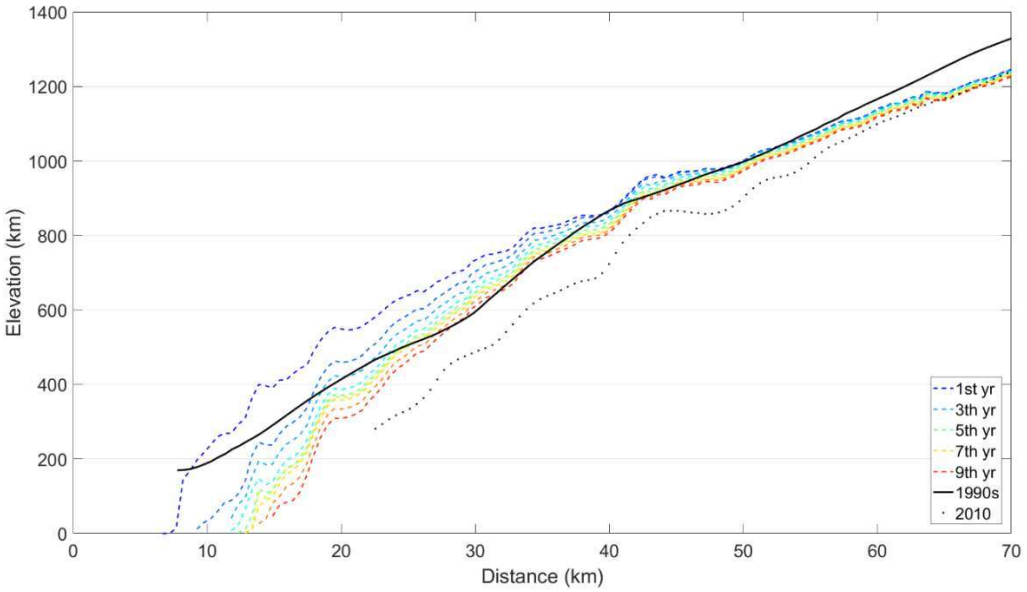

Figure S23. Profiles of surface elevation during the initialization procedure (section 2.3) step 3. Black solid line and black dashed line show the known profiles taken in the 1990s (Bamber et al., 2001) and 2010 (Gogineni et al., 2012) respectively. The profile with legend '1st yr' is the final state of section 2.3 step 2. The profile '7th yr' is the geometry rebuilt for 2004's Jakobshavn, which is the initial state for later simulations.

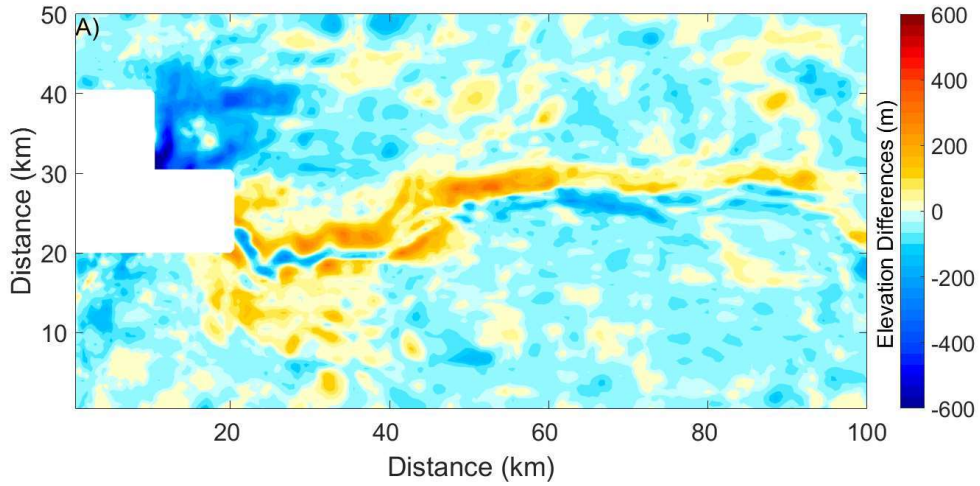

Figure S3. Bed elevation from BedMachine v3 (Morlighem et al., 2017) minus those from (Gogineni, 2012) used in this paper.